Summer 2013: No. 8

gacm Report

the german association for computational mechanics

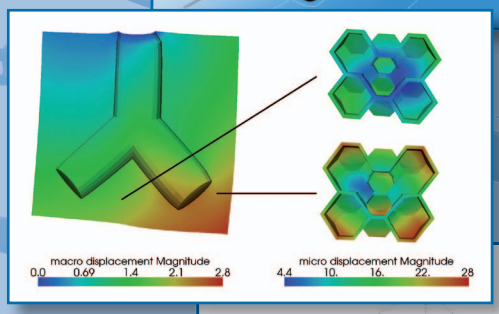

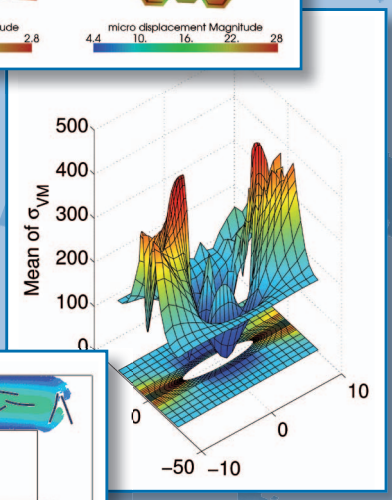

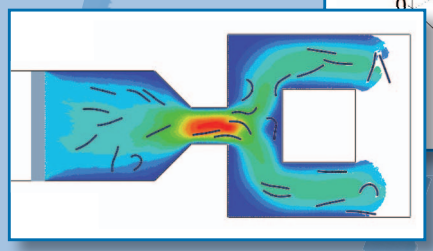

Algorithmic aspects of singularly perturbed multibody system models

M. Arnold

Topology Optimization in Flexible Multibody Dynamics

A. Held and R. Seifried

Soft structures with fluid interaction

M. Schörgenhumer, P.G. Gruber, K. Nachbagauer and J. Gerstmayr

Conferences

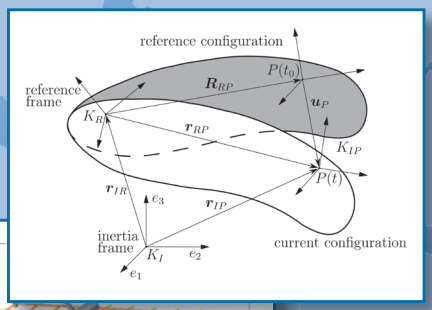

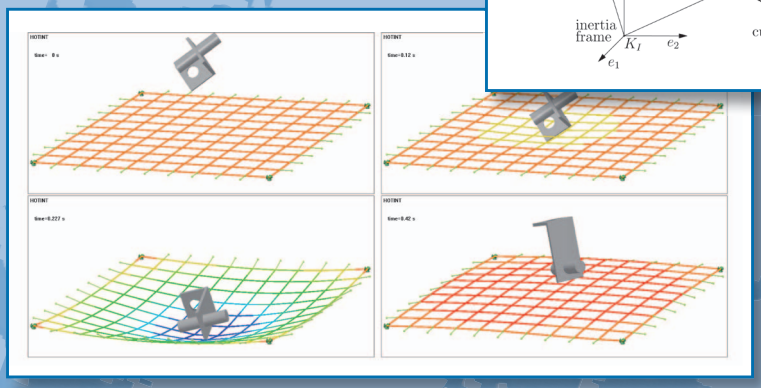

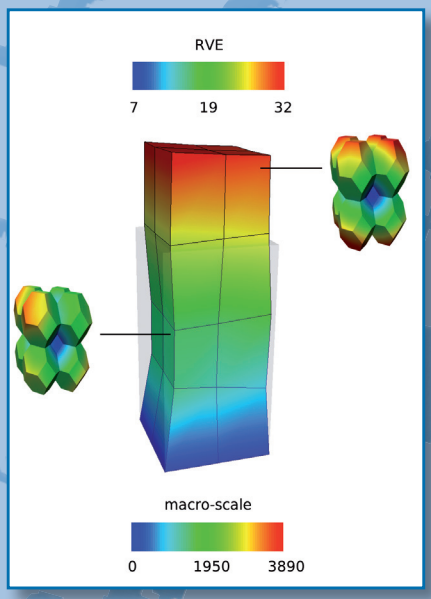

contents

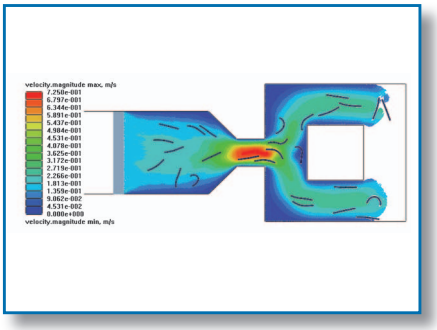

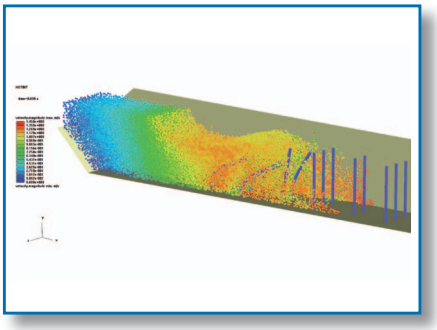

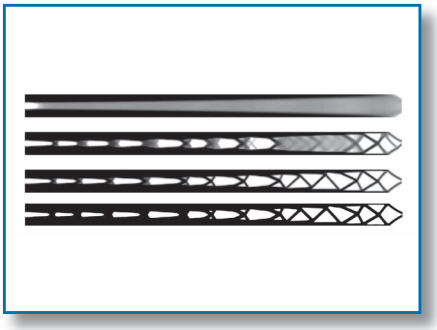

GACM-News

Journal

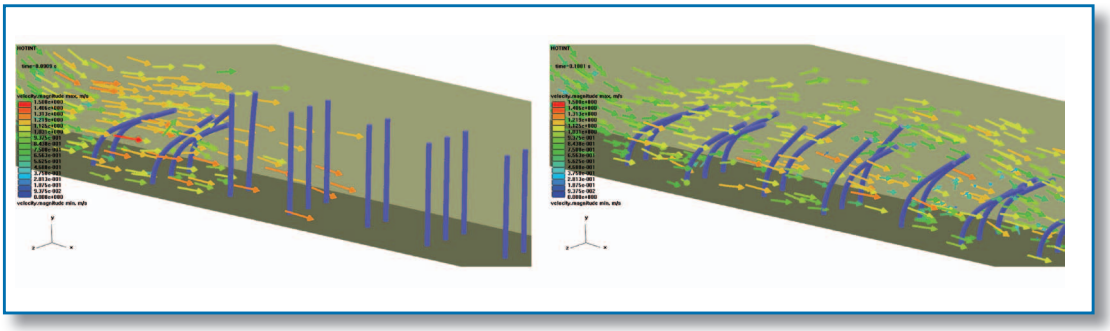

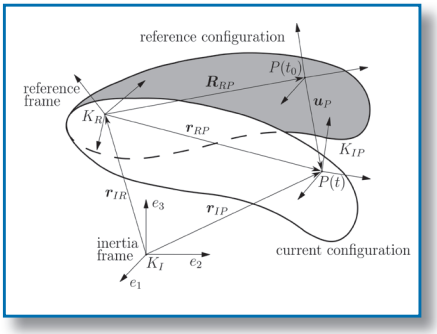

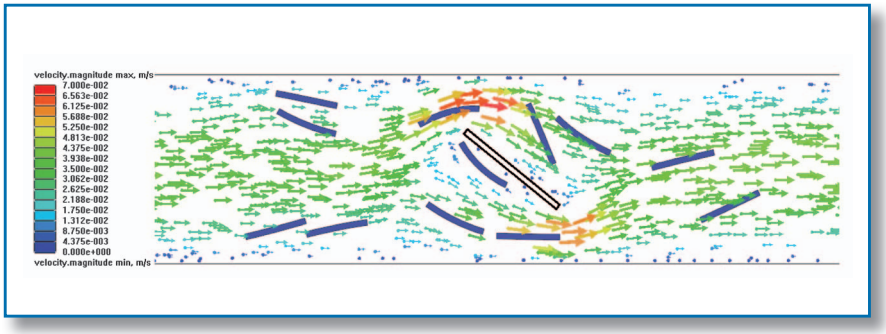

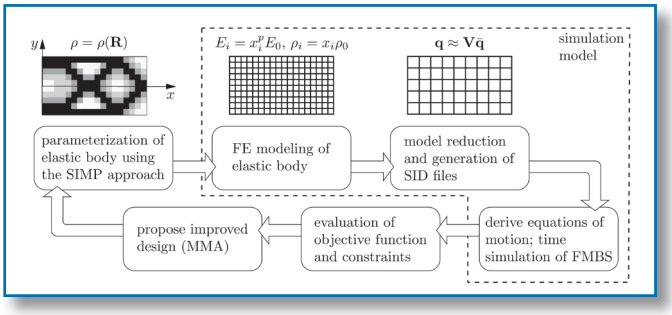

Conferences

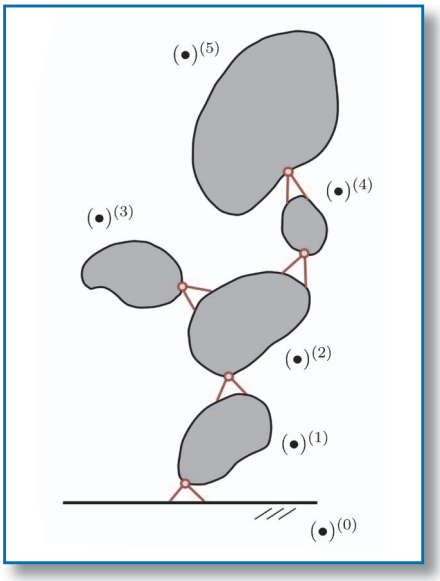

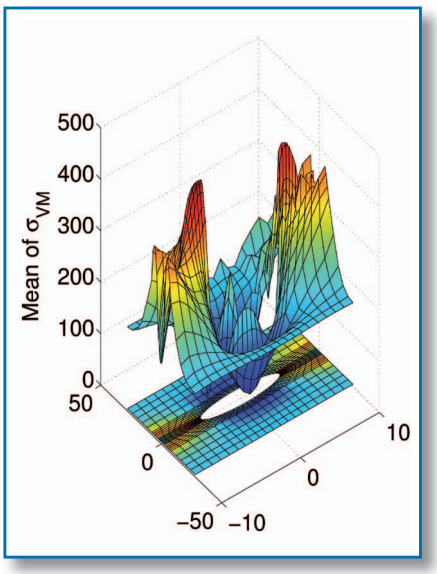

gacmReport

Publisher:
GACM
The German Association for Computational Mechanics

Address:
Institute for Computational Mechanics
Technische Universität München
Boltzmannstrasse 15
D-85747 Garching, Germany
Phone: +49 89 289-15300
Fax: +49 89 289-15301
email: gacm@lnm.mw.tum.de
Internet: www.gacm.de

Editor-in-Chief: Wolfgang A. Wall

Guest Editor: Sigrid Leyendecker

Grafik-Design & Print:
K. Schmidle Druck und Medien GmbH, Ebersberg

Print Run: 500

Editorial

The present issue of the GACM Report is the first one to be published within the four years office term of the new executive council, which has been elected at the last general meeting of the GACM in Vienna in September 2012. As usual, this report summarizes some relevant events that happened in our community of computational mechanics in Germany and abroad. These include awards and honors going to GACM members and the granting of the first GACM Award.

The actual GACM Report highlights some dynamical aspects within the field of computational mechanics. In particular, the scientific articles address the simulation of the dynamics of flexible multibody systems and the corresponding two major thematic conferences are presented shortly. Modeling the dynamic behaviour of interconnected rigid or flexible bodies that undergo large translational and rotational motion, multibody system dynamics is a branch of computational mechanics that becomes increasingly important in the development of complex technological systems. Having its roots in robotics, aeronautics and vehicle dynamics, the possibility to include any flexible body description and diverse models of interaction with the surroundings and control from the outside enables the application of multibody dynamics in a variety of fields ranging from biomechanics over multiscale and multiphysics problems to mechatronic systems. The development of more and more sophisticated numerical methods for the simulation of multibody dynamics provides a computational framework for their dynamic analysis as well as for the optimisation of system and process design.

This is illustrated by the three scientific articles in this report, developing first of all an efficient algorithm for the time integration of high frequency dynamics of systems containing bodies with small mass or nearly singular inertia tensor. The second paper demonstrates the application of topology optimization to the efficient design of flexible multibody systems such as lightweight manipulators and to improve their dynamical behavior. Finally, based on the framework of flexible multibody system dynamics and meshfree particle-based fluid mechanics, the interaction of a fluid with highly flexible fibers is predicted in the third article. Fluid-structure interaction plays an important role in various scientific and industrial fields, ranging from e.g. blood flow in biomechanics, wind-induced vibrations of buildings or bridges over the production of fiber-reinforced or composite materials to processes involving wave motion and free-surface flows.

The issue closes with reports on past conferences and an overview of relevant future conferences in computational mechanics and engineering.

August 2013

Sigrid Leyendecker
Chair of Applied Dynamics
University of Erlangen-Nuremberg

Message of the President

This is the first issue of our GACM report during the term of office of the new executive council and my recently commenced term as president. And it is not only a perfect occasion, but also my heartfelt wish to start with a number of acknowledgements.

First I would like to thank the outgoing president Peter Wriggers for his work over many years and his willingness to continue to be a member of the executive council for four more years, to share and hand on his insights and experiences. I also would like to thank all outgoing members of the executive council, namely Manfred Bischoff, Günter Meschke, Günther Müller and Werner Wagner, as well as the past Secretary General, Stefan Löhnert.

I am very grateful to the incoming members of the executive council for their willingness to serve our scientific community and to form a prosperous future for it through GACM. It is exciting to see successful members of the community taking responsibility for the whole and making it their personal concern. And what would a president be without an excellent Secretary General? Hence, I am particularly indebted to Lena Yoshihara and Alexander Popp for their willingness to accept this responsibility.

Finally, on behalf of the whole new executive council, I would like to thank all members of GACM for the confidence you have placed in us.

What and Why?

You might ask what GACM does and why such an association is necessary at all – and some people actually asked me these questions already several times over the years. Is it not enough to do good research and teaching, participate or even organize a conference, apply the most advanced techniques in industry, etc.? Well, if everyone thinks and acts like that, it probably would work and you would not notice too much of a difference – at least for a while. But then we probably would notice – just to name a few issues – that

– issues on the national and even more on the international level are not coordinated anymore;
– actually valuable and good conference series suddenly and unexpectedly stop;
– our scientific field – which is something that we believe is important for the future of our society – gradually forfeits its importance and visibility for funding agencies and other main players and decision makers;
– the German part of our scientific community, namely our points of view, our issues, etc., loose ground in the greater European or international community, respectively.

And just to make it clear: GACM definitely exists neither to share sinecures nor to give new honorary titles nor to fight other associations on being the superior one.

The main task of GACM is to serve our scientific community! This primary goal defines the agenda of the new executive council. I am particularly grateful that all EC members share this conviction. The new executive council already met twice in the meantime, having had several in-depth discussions on our potential activities and priorities for the upcoming four-year period. It is not necessary to list them here, since hopefully you will recognize them anyway.

One essential thing will be that many people really get involved. This will enable us to serve our community best. So my wish for all of you is:

GET INVOLVED!

Wolfgang A. Wall

New GACM Executive Council took office in January 2013

At the general meeting of GACM, that took place in September 2012, a new Executive Council has been elected unanomiously. The new team took office in January 2013 for a four year term according to the GACM bylaws. Wolfgang A. Wall from TU München, vice president of GACM in the last four years, has been elected as the new president and Michael Kaliske from TU Dresden has been elected as the new vice president.
Further members of the EC are:

Wolfgang A. Wall from TU München, has been elected as the new president

Michael Kaliske from TU Dresden has been elected as the new vice president

Marek Behr from RWTH Aachen (representing CFD and CSE),

Sven Klinkel from RWTH Aachen (Treasurer),

Sigrid Leyendecker from FAU Erlangen-Nürnberg (representing Mathematics and Dynamics),

Thomas Münz from DynaMore (representing industry) and

Peter Wriggers from LU Hannover (as past president).

Lena Yoshihara from TU München will act as the new Secretary General and during

her maternity leave she will be substituted by Alexander Popp from TU München.

Ekkehard Ramm elected as Honorary Chairman of GACM

During the last member assembly of the German Association of Computational Mechanics at the ECCOMAS Congress in Vienna in September 2012, Professor Ekkehard Ramm has been elected as Honorary Chairman of the Association. This very rare and special distinction has been unanonimously supported by the members of GACM and recognizes his dedicated and long time work for GACM.

Ekkehard Ramm was a GACM member from the very start of the Association and over the years has permanently served not only GACM but also the broader community in Computational Mechanics. He became President of GACM in 2000 and his two term service as President until 2008 marked a very fruitful time for GACM. Not only the number of full members grew substantially but also a number of new initiatives have been taken that are still in place today and by this form a kind of heritage of his presidency.

Two examples are the start of the GACM Report, and the beginning of a very successful and timely conference series – the GACM Colloquia for Young Scientists from Academia and Industry. These conferences and their success became the inspiration for a similar series on the European level, the ECCOMAS Young Investor Conference (YIC). Ekkehard Ramm also was very active on the European (within ECCOMAS) and the international level (IACM) where he not only represented GACM interests. He not at all served his personal interests but always had a broader, holistic point of view; he always works for a sustained development of the community. The GACM Executive Council is happy to enjoy his advise also in the future.

GACM Award goes to Dr. Bojana Rosic

For the first time, the GACM awards a price for the best PhD thesis in Germany. The award goes to Dr. Bojana Rosić, who will also be nominated as a candidate for the next round of the ECCOMAS PhD award.

Dr. Bojana Rosić, born in 1982, has completed her engineering studies in 2006 at the University of Kragujevac in Serbia. Both in school and at university she has won several prizes. Between 2007 and 2012 she was in a joint doctoral programme between the University of Kragujevac and the TU Braunschweig. She defended her thesis on "Variational Formulations and Functional Approximation Algorithms in Stochastic Plasticity of Materials" in November 2012, achieving the highest distinction "summa cum laude".

The developments contained in her thesis allow the "quantification of uncertainty" of elasto-plastic systems at infinitesimal and finite strains, where both the elastic and plastic behavior are characterized by possibly inhomogeneous and anisotropic random tensor fields.

In her work, Dr. Rosić has covered the ground from abstract theoretical existence proofs all the way to practical intrusive and non-intrusive variants of stochastic discretizations, which have already caught the interest of industry.

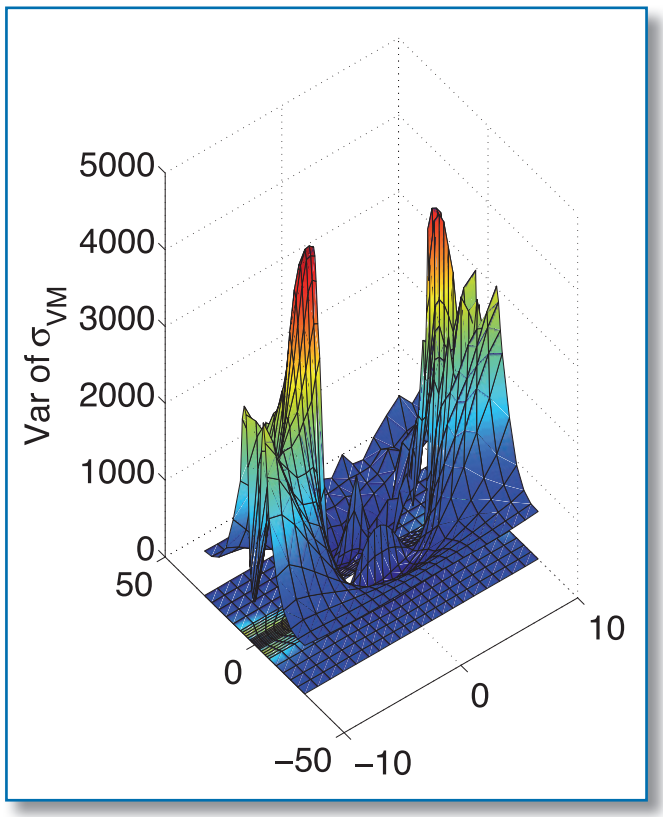

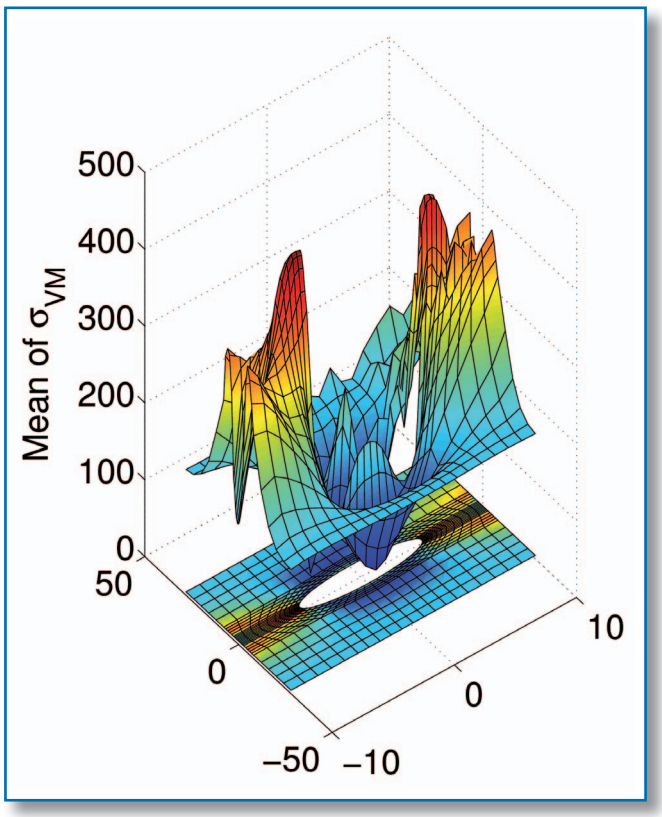

Prestigious European Awards go to GACM Members

2012 marked a very successful year for GACM as the following two impressive examples demonstrate.

Prof. em. Dr.-Ing. habil. Dr.-Ing. E.h. Dr. h.c. mult. Erwin Stein, from the Leibniz University Hannover, received the highest award given by ECCOMAS, namely the Ritz-Galerkin medal. The award ceremony took place at the opening of the ECCOMAS congress in September 2012 in the main concert hall of the Vienna Musikverein.

Another reason for celebration for GACM was the fact that the ECCOMAS PhD award for the best PhD thesis in the field of Computational Methods in Applied Sciences and Engineering went to an awardee from Germany for the first time.

Dr.-Ing. Lena Wiechert (now Yoshihara) from Technische Universität München received this award for her thesis entitled "Computational modeling of multi-field and multi-scale phenomena in respiratory mechanics".

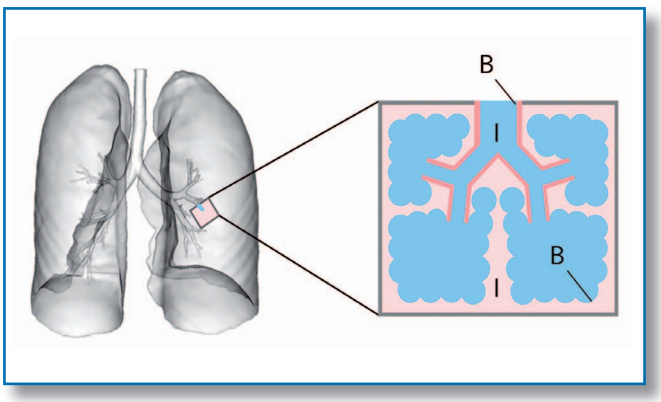

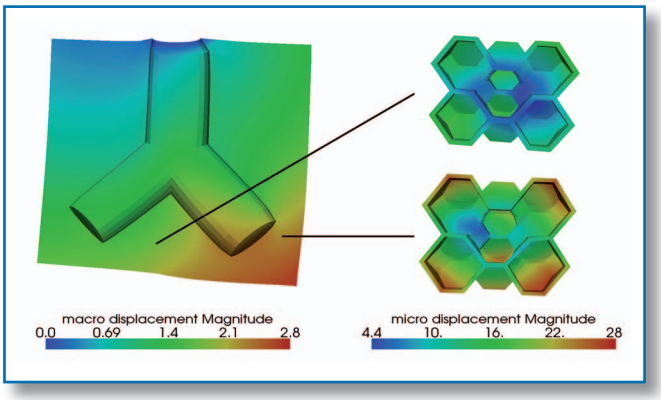

Algorithmic aspects of singularly perturbed multibody system models

M. Arnold
Institute of Mathematics, Martin Luther University Halle-Wittenberg

Abstract

Complex multibody system models that contain bodies with small mass or nearly singular inertia tensor may suffer from high frequency solution components that deteriorate the solver efficiency in time integration. Singular perturbation theory suggests to neglect these small mass and inertia terms to allow a more efficient computation of the smooth solution components. In the present paper, a recursive multibody formalism is developed to evaluate the equations of motion for a tree structured N body system with O(N) complexity even if isolated bodies have a rank-deficient body mass matrix.

1 Introduction

Classical time integration methods in technical simulation are tailored to problems with smooth solution. Small system parameters may introduce rapidly oscillating or strongly damped solution components that cause problems in time integration. Singular perturbation theory gives much insight in the analytical background of these phenomena and allows furthermore an efficient approximation of *smooth* solutions neglecting all terms that contain small parameters, see, e.g., [8].

The application of these classical results to multibody dynamics is non-trivial since the numerical algorithms for evaluating the equations of motion efficiently (multibody formalisms) are based on regularity assumptions that may be violated if small mass and inertia terms are neglected. In the present paper, we give an overview on singularly perturbed problems in multibody dynamics (Section 2) and focus on algorithmic aspects of this approach. In Section 3, a recursive multibody formalism is introduced that may be extended to multibody system models with rank deficient body mass matrices. Following step by step the analysis of [1], the details of this extension are discussed in Section 4.

2 Singularly perturbed problems

In this paper, our main interest is in multibody system models with small mass and inertia terms. Related problems are, e.g., the modelling of serial spring-damper elements using an auxiliary zero mass body between spring and damper [3, Section 1.3.4], the modifcation of inertia forces for high-frequency eigenmodes of fexible bodies in multibody system models for the analysis of elastohydrodynamic bearing coupling in [13] and some methods from FE contact mechanics in [7]. For real-time applications in multibody dynamics, the inertia forces of small mass bodies were neglected by [4]. A more detailed analysis shows, that this approach is straightforward if all small mass bodies of the multibody system are leaf bodies in the kinematic tree. In numerical experiments for the model of a walking mobile robot (mobot) with stiff contact forces between lightweight legs and ground floor, the numerical effort was reduced by a factor of 4, see [15].

2.1 The reduced problem

The research on singularly perturbed multibody system models is guided by well known results from general singular perturbation theory, see [8], and its extensions to second order differential equations by Lubich et al., see [9] and [14]. The generic form of singularly perturbed ordinary differential equations (ODEs) are partitioned systems

$$\dot{\boldsymbol{y}}_\varepsilon = \boldsymbol{\varphi}(\boldsymbol{y}_\varepsilon, \boldsymbol{z}_\varepsilon) \quad (1a)$$
$$\varepsilon\dot{\boldsymbol{z}}_\varepsilon = \boldsymbol{\gamma}(\boldsymbol{y}_\varepsilon, \boldsymbol{z}_\varepsilon) \quad (1b)$$

with a small perturbation parameter $\varepsilon > 0$ that are considered at a fnite time interval $[0,t_e]$, see [8, Chapter VI] and the references therein.

For any given initial value $\boldsymbol{y}^0$, the singularly perturbed system (1) has a smooth solution $(\boldsymbol{y}_\varepsilon^0(t), \boldsymbol{z}_\varepsilon^0(t))$ with $\boldsymbol{y}_\varepsilon^0(0) = \boldsymbol{y}^0$ if the right hand side of the singularly perturbed subsystem (1b) has a Jacobian with eigenvalues satisfying along each solution trajectory $(\boldsymbol{y}_\varepsilon(t), \boldsymbol{z}_\varepsilon(t))$ the condition

$$\mathrm{Re}\,\lambda_i\,[(\partial\boldsymbol{\gamma}/\partial\boldsymbol{z}_\varepsilon)(\boldsymbol{y}_\varepsilon, \boldsymbol{z}_\varepsilon)] \le -\beta < 0$$

for some positive constant $\beta > 0$. This smooth solution remains in an $O(\varepsilon)$-neighbourhood of the solution $(\boldsymbol{y}_0(t), \boldsymbol{z}_0(t))$ of the *reduced problem* that results from setting formally the perturbation parameter in (1) to $\varepsilon := 0$. We get

$$\dot{\boldsymbol{y}}_0 = \boldsymbol{\varphi}(\boldsymbol{y}_0, \boldsymbol{z}_0)\,, \quad (2a)$$
$$\boldsymbol{0} = \boldsymbol{\gamma}(\boldsymbol{y}_0, \boldsymbol{z}_0) \quad (2b)$$

with $\boldsymbol{y}_0(0) = \boldsymbol{y}^0$ and $\boldsymbol{z}_0(0)$ being implicitly defined by (2b). The general solution of the singularly perturbed problem (1) has the form

$$\boldsymbol{\gamma}_\varepsilon(t) = \boldsymbol{\gamma}_\varepsilon^0(t) + \varepsilon\boldsymbol{\eta}_\varepsilon\,(t/\varepsilon) = \boldsymbol{\gamma}_0(t) + O(\varepsilon), \qquad (3a)$$

$$\boldsymbol{z}_\varepsilon(t) = \boldsymbol{z}_\varepsilon^0(t) + \boldsymbol{\zeta}_\varepsilon(t/\varepsilon) = \boldsymbol{z}_0(t) + O(\varepsilon) + \boldsymbol{\zeta}_\varepsilon(t/\varepsilon) \qquad (3b)$$

with smooth functions $\boldsymbol{\eta}_\varepsilon(t/\varepsilon)$, $\boldsymbol{\zeta}_\varepsilon(t/\varepsilon)$ that decay like $\exp(-\bar{\beta}t/\varepsilon)$ for some positive constant $\bar{\beta} \in (0,\beta)$, see [8, Theorem VI.3.2].

For many stiff integrators, the numerical solution of (1) may be decomposed as well in a smooth part and a rapidly decaying part reflecting the transient behaviour for initial values $(\boldsymbol{\gamma}_\varepsilon(0), \boldsymbol{z}_\varepsilon(0))$ that do not belong to a smooth solution. If there is no particular interest in this transient phase, an approximate numerical solution may be obtained much more efficiently solving for given initial values $\boldsymbol{\gamma}_0(0) := \boldsymbol{\gamma}_\varepsilon(0)$ the reduced problem (2) by appropriate time integration methods for differential algebraic equations (DAEs) [8, Chapter VI]. Note, that the initial values $\boldsymbol{z}_0(0)$ in DAE (2) are not free but have to satisfy $\boldsymbol{\gamma}(\boldsymbol{\gamma}_0(0), \boldsymbol{z}_0(0)) = \boldsymbol{0}$.

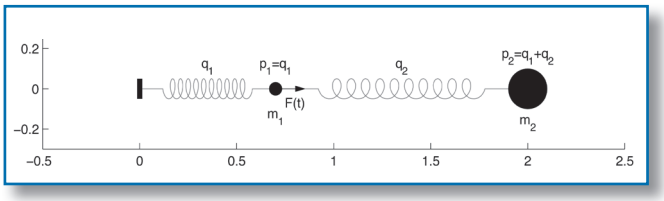

Figure 1:
Coupled oscillators with a fast oscillating small mass m_1, see [2].

Lubich [9] extended these classical results to a class of singular singularly perturbed problems

$$M(\boldsymbol{q})\ddot{\boldsymbol{q}} = \psi(\boldsymbol{q},\dot{\boldsymbol{q}}) - \frac{1}{\varepsilon^2}\nabla U(\boldsymbol{q}) \qquad (4)$$

with $\boldsymbol{q}(t)$ denoting the position coordinates of a multibody system. Matrix $\mathbf{M}(\boldsymbol{q})$ is the symmetric positive definite mass matrix and $\boldsymbol{\psi}(\boldsymbol{q}, \dot{\boldsymbol{q}})$ denotes a vector of forces and momenta. The crucial term in (4) are the (very) stiff potential forces $-\varepsilon^{-2}\nabla U(\boldsymbol{q})$ that depend on the perturbation parameter ε with $0 < \varepsilon \ll 1$. If the potential $U(\boldsymbol{q})$ attains a local minimum on a manifold $\mathcal{U}$ and is strongly convex along all directions that are non-tangential to $\mathcal{U}$, then the smooth solution of (4) may be approximated up to $O(\varepsilon^2)$ by the solution $\boldsymbol{q}_0(t)$ of a constrained (differential-algebraic) system with $\boldsymbol{q}_0(t) \in \mathcal{U}, (t \geq 0)$. In general, this constrained system may be solved much more efficiently than the original singularly perturbed problem (4), see [8].

In [14], these results were extended to mechanical systems with strong damping forces $-\varepsilon^{-1}\mathbf{D}(\boldsymbol{q})\dot{\boldsymbol{q}}$ in the right hand side of (4). In the limit case $\varepsilon \to 0$, the solution of the singularly perturbed problem is again approximated by the solution of a DAE problem that can be obtained in a robust and efficient way by standard DAE time integration methods, see [8].

In the present paper we focus on the numerical solution of the reduced problem (2) to get the zero order approximation $\boldsymbol{z}_0(t)$ for the smooth solution $\boldsymbol{z}_\varepsilon^0(t)$ efficiently. But from the practical viewpoint, higher order approximations

$$\boldsymbol{z}_\varepsilon^0(t) = \boldsymbol{z}_0(t) + \varepsilon\boldsymbol{z}_1(t) + \ldots + \varepsilon^r\,\boldsymbol{z}_r(t) + O(\varepsilon^{r+1})$$

are interesting as well since in that way the dynamics of the slowly varying subsystem (1a) may be approximated by $\dot{\boldsymbol{\gamma}}_\varepsilon = \boldsymbol{\varphi}(\boldsymbol{\gamma}_\varepsilon, \boldsymbol{z}_\varepsilon^0)$ up to terms of order $O(\varepsilon^{r+1})$. Recently, Gorius et al. [6] proposed such an inertial manifold approach [11] to design an approximate feedforward control of fexible multibody systems.

2.2 Motivating example: The small mass oscillator

The eigenfrequency of a harmonic oscillator is given by $\omega = \sqrt{c/m}$ with mass m and spring constant c. High frequency oscillations in a mechanical system may not only be introduced by (very) stiff potential forces but also by potential forces of moderate size that act on a body with (very) small mass.

In [2], this phenomenon was studied for the simple model problem in Fig. 1. In two coupled oscillators, a small mass m_1 is connected to a large mass m_2 and to the reference system by stiff springs with constants c_1, c_2 and damping with damping parameters d_1, d_2. Both bodies can only move along the x-axis. Additional forces $F(t)$ are only acting on m_1. In absolute coordinates $\boldsymbol{p}(t)=(p_1(t),p_2(t))^\top$, the equations of motion are given by

$$m_1\ddot{p}_1 = F(t) - d_1\dot{p}_1 - c_1p_1 + d_2(\dot{p}_2 - \dot{p}_1) + c_2(p_2 - p_1)\,, \qquad (5a)$$

$$m_2\ddot{p}_2 = -d_2(\dot{p}_2 - \dot{p}_1) - c_2(p_2 - p_1)\,. \qquad (5b)$$

The small mass can oscillate very fast depending on the ratio of the masses and spring parameters. If the perturbation parameter $\varepsilon :=$

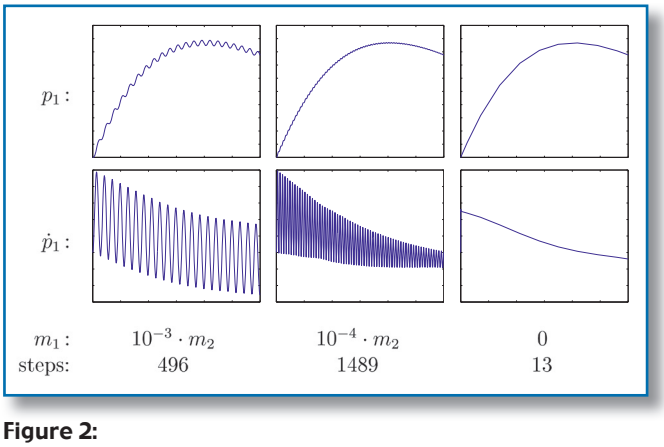

Figure 2:
Simulation results for decreasing mass ratios m_1/m_2, see [2].

m_1 gets smaller, the frequency of the oscillations increases and a time integration method with stepsize control would choose very small stepsizes to resolve these oscillations and meet the integration tolerances. The number of time steps and the computing time increase signifcantly. In Fig. 2 the number of time steps of the BDF solver DASSL with tolerances 10^{-6} for absolute and relative errors is given for decreasing mass ratios m_1/m_2. In the limit case $\varepsilon = m_1 = 0$, the inertia forces of the first mass point are neglected and (5a) results in an implicit first order differential equation

$$0 = F(t) - d_1\dot{p}_1 - c_1p_1 + d_2(\dot{p}_2 - \dot{p}_1) + c_2(p_2 - p_1) \ . \qquad (6)$$

The fast oscillations of the small mass disappear and the integrator can use large stepsizes, see Fig. 2.

In a description by relative coordinates $\boldsymbol{q}(t)=(q_1(t),q_2(t))^\top$ with $p_1(t) =: q_1(t)$ and $p_2(t) - p_1(t) =: q_2(t)$, the limit process $\varepsilon \to 0$ causes substantial problems since the equations of motion (5b) of the *large mass* depend on $\ddot{p}_2 = \ddot{q}_1 + \ddot{q}_2$ but $\ddot{q}_1 = \ddot{p}_1$ does not appear in (6). Furthermore, the diferentiation of (6) w.r.t. time t shows that $\ddot{q}_1(t)$ depends on the time derivative of $F(t)$ in the limit case $\varepsilon = m_1 = 0$.

3 A recursive multibody formalism for systems with tree structure

We describe the confguration of the multibody system by the absolute position and orientation of all N bodies relative to the inertial frame and use joint coordinates as generalized coordinates for a tree structured system ("mixed coordinates"), see also [12]. For tree structured systems, the joint accelerations may be obtained by a sequence

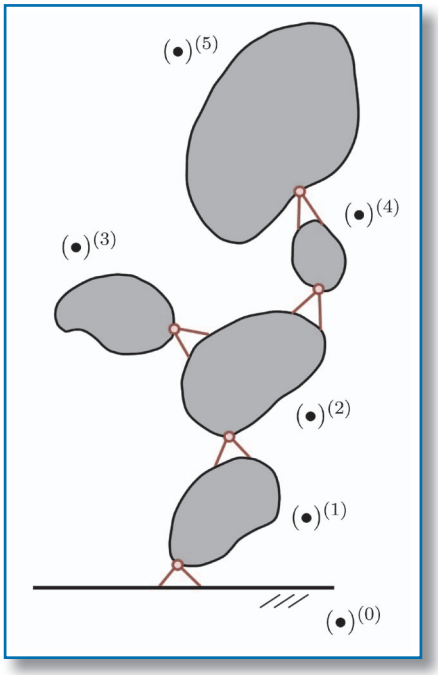

Fig. 3:
Tree structured multibody system.

of recursively defined computations that are known as *multibody formalism* ("O(N)-formalism"). As in [10] and [3], this recursive multibody formalism is interpreted as a block Gaussian elimination for a sparse, (very) large blockstructured system of linear equations with the block structure being determined by the topology of the multibody system.

Recursive multibody formalisms are tailored to tree structured systems. Here, the term tree *structure* corresponds to the structure of the labelled graph being associated to the multibody system model. In this graph, each (rigid or fexible) body of the system is represented by a vertex. Two vertices of the graph are connected by an edge if and only if the corresponding bodies in the multibody system model are connected by a joint restricting their relative motion.

The graph of a tree structured multibody system is acyclic, i.e., it is free of loops. Then, the multibody system has a *root* body $(\bullet)^{(0)}$ that corresponds to the root vertex of the tree structured graph and is supposed to be inertially fixed. All other bodies $(\bullet)^{(i)}$ have a uniquely defined predecessor $(\bullet)^{(\pi_i)}$ in the kinematic tree. Each body $(\bullet)^{(i)}$ may have successors $(\bullet)^{(j)}$ being characterized by $\pi_j = i$ or, equivalently, by $j \in I_i := \{ k : \pi_k = i \}$ with an index set I_i that represents the set of all successors of a given body $(\bullet)^{(i)}$ in the multibody system model. Bodies without successors ($I_i = \emptyset$) correspond to leafs of the kinematic tree and are therefore called leaf bodies.

For the configuration in Fig. 3, we have the inertially fixed root body $(\bullet)^{(0)}$ and $N = 5$ bodies $(\bullet)^{(i)}$, ($i = 1, \ldots, 5$), with

$$\pi_1 = 0,\ \pi_2 = 1,\ \pi_3 = 2,\ \pi_4 = 2,\ \pi_5 = 4$$

and

$$I_1 = \{ 2 \},\ I_2 = \{ 3, 4 \},\ I_3 = \emptyset\ ,\ I_4 = \{ 5 \},\ I_5 = \emptyset\ ,$$

i.e., body $(\bullet)^{(i)}$ is the only direct successor of the root body $(\bullet)^{(0)}$ and the leaf bodies are $(\bullet)^{(3)}$ and $(\bullet)^{(5)}$.

We suppose that position and orientation of body $(\bullet)^{(i)}$ may be characterized by (absolute) position coordinates $\boldsymbol{p}_i(t) \in \mathbb{R}^d$ with $d = 6$ for 3D models and $d = 3$ for 2D models. The *relative* position and orientation of body $(\bullet)^{(i)}$ w.r.t. its predecessor $(\bullet)^{(\pi_i)}$ is characterized by joint coordinates $\boldsymbol{q}_i(t) \in \mathbb{R}^{n_i}$ representing the n_i degrees of freedom of the joint connecting $(\bullet)^{(i)}$ with $(\bullet)^{(\pi_i)}$:

$$\mathbf{0} = \boldsymbol{k}_i(\boldsymbol{p}_i, \boldsymbol{p}_{\pi_i}, \boldsymbol{q}_i, t) \ . \qquad (7)$$

Here and in the following we suppose that (7) is locally uniquely solvable w.r.t. $\boldsymbol{p}_i$ and that the Jacobian $\mathbf{K}_i = \partial \boldsymbol{k}_i / \partial \boldsymbol{p}_i$ is nonsingular along the solution. In its most simple form, Eq. (7) defines $\boldsymbol{p}_i$ explicitly by $\boldsymbol{p}_i(t) = \boldsymbol{r}_i(\boldsymbol{p}_{\pi_i}(t), \boldsymbol{q}_i(t), t)$ resulting in $\mathbf{K}_i = \mathbf{I}_d$.

The kinematic relations (7) at the level of position coordinates imply relations at the level of

velocity and acceleration coordinates that may formally be obtained by (total) diferentiation of (7) w.r.t. time t:

$$\mathbf{0} = \frac{\mathrm{d}}{\mathrm{d}t}\boldsymbol{k}_i(\boldsymbol{p}_i(t), \boldsymbol{p}_{\pi_i}(t), \boldsymbol{q}_i(t), t) \quad (8)$$
$$= \mathbf{K}_i\dot{\boldsymbol{p}}_i + \mathbf{H}_i\dot{\boldsymbol{p}}_{\pi_i} + \mathbf{J}_i\dot{\boldsymbol{q}}_i + \boldsymbol{k}_i^{(\mathrm{I})}(\boldsymbol{p}_0, \boldsymbol{p}, \boldsymbol{q}, t)\,,$$

$$\mathbf{0} = \mathbf{K}_i\ddot{\boldsymbol{p}}_i + \mathbf{H}_i\ddot{\boldsymbol{p}}_{\pi_i} + \mathbf{J}_i\ddot{\boldsymbol{q}}_i + \quad (9)$$
$$\boldsymbol{k}_i^{(\mathrm{II})}(\boldsymbol{p}_0, \dot{\boldsymbol{p}}_0, \boldsymbol{p}, \dot{\boldsymbol{p}}, \boldsymbol{q}, \dot{\boldsymbol{q}}, t)$$

with

$$\mathbf{K}_i := \frac{\partial \boldsymbol{k}_i}{\partial \boldsymbol{p}_i} \in \mathbb{R}^{d\times d}\,, \quad \mathbf{H}_i := \frac{\partial \boldsymbol{k}_i}{\partial \boldsymbol{p}_{\pi_i}} \in \mathbb{R}^{d\times d}\,,$$
$$\mathbf{J}_i := \frac{\partial \boldsymbol{k}_i}{\partial \boldsymbol{q}_i} \in \mathbb{R}^{d\times n_i}\,.$$

It is supposed that the joint coordinates $\boldsymbol{q}_i(t)$ are defined such that all Jacobians $\mathbf{J}_i$ have full column rank: rank $\mathbf{J}_i = n_i \le d$.

Functions $\boldsymbol{k}_i^{(I)} = \partial\boldsymbol{k}_i/\partial t$ and $\boldsymbol{k}_i^{(II)}$ summarize partial time derivatives and all lower order terms in the first and second time derivative of (7), respectively. They may depend on the (absolute) coordinates $\boldsymbol{p}_0$ of the root body, on the absolute coordinates $\boldsymbol{p} := (\boldsymbol{p}_1,\ldots, \boldsymbol{p}_N)$ of the remaining N bodies in the system, on the corresponding joint coordinates $\boldsymbol{q} := (\boldsymbol{q}_1,\ldots, \boldsymbol{q}_N)$ and on $\dot{\boldsymbol{p}}_0$, $\dot{\boldsymbol{p}}$ and $\dot{\boldsymbol{q}}$. Note, that the root body is inertially fixed resulting in $\ddot{\boldsymbol{p}}_0 = \mathbf{0}$.

In recursive multibody formalisms, it is supposed that position and velocity of the root body $(\boldsymbol{p}_0(t), \dot{\boldsymbol{p}}_0(t))$ and all joint coordinates $\boldsymbol{q}_i(t)$, $\dot{\boldsymbol{q}}_i(t)$, $(i = 1,\ldots,N)$, at a current time t are known. Starting from the root body, the absolute position and velocity coordinates $\boldsymbol{p}_1(t)$, $\dot{\boldsymbol{p}}_1(t)$ of all N bodies $(\bullet)^{(i)}$, $(i = 1,\ldots,N)$, may then be computed recursively using (7) and (8), respectively. For the multibody system model in Fig. 3, this *forward recursion* starts at body $(\bullet)^{(1)}$ taking into account $\boldsymbol{p}_{\pi_1} = \boldsymbol{p}_0$, $\dot{\boldsymbol{p}}_{\pi_1} = \dot{\boldsymbol{p}}_0$. With $\boldsymbol{p}_1$ and $\dot{\boldsymbol{p}}_1$ being implicitly defined by (7) and (8), we may compute $\boldsymbol{p}_2$, $\dot{\boldsymbol{p}}_2$ by (7) and (8) with $i = 2$ and $\boldsymbol{p}_{\pi_2} = \boldsymbol{p}_1$, $\dot{\boldsymbol{p}}_{\pi_2} = \dot{\boldsymbol{p}}_1$. The forward recursion proceeds with $\boldsymbol{p}_3$, $\dot{\boldsymbol{p}}_3$ in the left branch of the tree and with $\boldsymbol{p}_4$, $\dot{\boldsymbol{p}}_4$, $\boldsymbol{p}_5$, $\dot{\boldsymbol{p}}_5$ in its right branch.

The equations of motion of a multibody system with N bodies may be obtained from the equilibrium conditions for forces and momenta for each individual body that are formulated in absolute coordinates $\boldsymbol{p}_i$:

$$\mathbf{M}_i\ddot{\boldsymbol{p}}_i + \mathbf{K}_i^{\top}\boldsymbol{\mu}_i + \sum_{j\in I_i}\mathbf{H}_j^{\top}\boldsymbol{\mu}_j = \quad (10)$$
$$\boldsymbol{f}_i\,,\ (i = 1,\ldots,N)\,.$$

The body mass matrix $\mathbf{M}_i \in \mathbb{R}^{dxd}$ contains mass and inertia tensor of body $(\bullet)^{(i)}$ and is supposed to be symmetric, positive semi-definite. The equilibrium conditions contain the reaction forces of the joints connecting body $(\bullet)^{(i)}$ with its predecessor $(\mathbf{K}_i^{\top}\boldsymbol{\mu}_i)$ and with its successors in the kinematic tree $(\mathbf{H}_j^{\top}\boldsymbol{\mu}_j, j \in I_i)$. All remaining forces and momenta acting on body $(\bullet)^{(i)}$ are summarized in the force vector $\boldsymbol{f}_i = \boldsymbol{f}_i(\boldsymbol{p}, \dot{\boldsymbol{p}}, \boldsymbol{q}, \dot{\boldsymbol{q}}, t) \in \mathbb{R}^d$. The specific structure of the joint reaction forces with Lagrange multipliers $\boldsymbol{\mu}_i(t) \in \mathbb{R}^d$ that satisfy

$$\mathbf{J}_i^{\top}\boldsymbol{\mu}_i = \mathbf{0}\,,\ (i = 1,\ldots,N)\,, \quad (11)$$

results from the joint equations (7) and from d'Alembert's principle since the virtual work of constraint forces vanishes for all (virtual) displacements being compatible with (7). In (11), matrix $\mathbf{J}_i$ denotes again the Jacobian of the constraint function $\boldsymbol{k}_i$ w.r.t. joint coordinates $\boldsymbol{q}_1 \in \mathbb{R}^{n_i}$.

For leaf bodies $(\bullet)^{(i)}$, the equilibrium conditions (10) get a simpler form since $I^i = \{\, j : \pi_j = i \,\} = \emptyset$. We obtain

$$\bar{\mathbf{M}}_i\mathbf{K}_i\ddot{\boldsymbol{p}}_1 + \boldsymbol{\mu}_i = \bar{\boldsymbol{f}}_i \quad (12)$$

with $\bar{\boldsymbol{f}}_i$, $\mathbf{K}_i^{-\mathrm{T}}\boldsymbol{f}_i$, $\mathbf{K}_i^{-\mathrm{T}} := (\mathbf{K}_i^{-1})^{-1}$ and the symmetric, positive semi-definite mass matrix $\bar{\mathbf{M}}_i := \mathbf{K}_i^{-\mathrm{T}}\mathbf{M}_i\mathbf{K}_i^{-1}$.

One of the basic components of recursive multibody formalisms are algorithms to transform the equilibrium conditions (10) recursively for *all* bodies $(\bullet)^{(i)}$ to the simpler form (12) with suitable $\bar{\mathbf{M}}_i$ and $\bar{\boldsymbol{f}}_i$. With the common assumption that all body mass matrices $\mathbf{M}_i$ are non-singular, $\boldsymbol{\mu}_i$ may be expressed in terms of $\ddot{\boldsymbol{p}}_{\pi_i}$, $\bar{\mathbf{M}}_i$, $\bar{\boldsymbol{f}}_i$ and $\boldsymbol{k}_i^{(II)}$ by block Gaussian elimination applied to (9), (11) and (12), see [10]. Using the resulting expressions for $\boldsymbol{\mu}_j$ for all successor bodies $(\bullet)^{(j)}$ of a given body $(\bullet)^{(i)}$, the equations of motion (10) may be transformed to the simpler form (12) with

$$\bar{\mathbf{M}}_i := \mathbf{K}_i^{-\mathrm{T}}\mathbf{M}_i\mathbf{K}_i^{-1} + \quad (13a)$$
$$+ \sum_{j\in I_i}\mathbf{K}_i^{-\mathrm{T}}\mathbf{H}_j^{\top}$$
$$(\bar{\mathbf{M}}_j - \bar{\mathbf{M}}_j\mathbf{J}_j(\mathbf{J}_j^{\top}\bar{\mathbf{M}}_j\mathbf{J}_j)^{-1}\mathbf{J}_j^{\top}\bar{\mathbf{M}}_j)\mathbf{H}_j\mathbf{K}_i^{-1}\,,$$

$$\bar{\boldsymbol{f}}_i := \mathbf{K}_i^{-\mathrm{T}}\boldsymbol{f}_i - \quad (13b)$$
$$- \sum_{j\in I_i}\mathbf{K}_i^{-\mathrm{T}}\mathbf{H}_j^{\top}$$
$$(\mathbf{I}_d - \bar{\mathbf{M}}_j\mathbf{J}_j(\mathbf{J}_j^{\top}\bar{\mathbf{M}}_j\mathbf{J}_j)^{-1}\mathbf{J}_j^{\top})(\bar{\boldsymbol{f}}_j + \bar{\mathbf{M}}_j\boldsymbol{k}_j^{(\mathrm{II})})\,,$$

see [1]. The condensed body mass matrix $\bar{\mathbf{M}}_i$ is a sum of symmetric positive semidefinite matrices. For non-singular body mass matrices $\mathbf{M}_i$, the condensed body mass matrix $\bar{\mathbf{M}}_i$ is non-singular as well.

For the tree structured multibody system model in Fig. 3, the *backward recursion* starts at the leaf bodies $(\bullet)^{(3)}$ and $(\bullet)^{(5)}$ since $I_3 = I_5 = \emptyset$ and $\bar{\mathbf{M}}_3$, $\bar{\boldsymbol{f}}_3$, $\bar{\mathbf{M}}_5$, $\bar{\boldsymbol{f}}_5$ may be obtained straightforwardly from (13). In the next step, the backward recursion follows the right branch of the tree structured model to evaluate $\bar{\mathbf{M}}_4$, $\bar{\boldsymbol{f}}_4$ according to (13) with $i = 4$ and $I_4 = \{5\}$. For the ramification vertex $(\bullet)^{(2)}$, we have $I_2 = \{3, 4\}$ and both right hand sides in (13) consist of three terms. Finally, $\bar{\mathbf{M}}_1$, $\bar{\boldsymbol{f}}_1$ are obtained from (13) with $i = 1$ and $I_1 = \{2\}$.

The second time derivative (9) of the kinematic relations (7) defines the acceleration $\ddot{\boldsymbol{p}}_i$ of body $(\bullet)^{(i)}$ in terms of the acceleration $\ddot{\boldsymbol{p}}_{\pi_i}$ of its predecessor $(\bullet)^{(\pi i)}$ and in terms of the corresponding joint

accelerations $\ddot{\boldsymbol{q}}_i$. To eliminate the joint accelerations $\ddot{\boldsymbol{q}}_i$, we multiply (9) from the left by $\mathbf{J}_i^\top \bar{\mathbf{M}}_i$ resulting in

$$(\mathbf{J}_i^\top \bar{\mathbf{M}}_i \mathbf{J}_i)\, \ddot{\boldsymbol{q}}_i = -\mathbf{J}_i^\top \bar{\mathbf{M}}_i (\mathbf{H}_i \ddot{\boldsymbol{p}}_{\pi i} + \boldsymbol{k}_i^{(II)}) - \mathbf{J}_i^\top \bar{\boldsymbol{f}}_i$$

since (14)

$$\mathbf{J}_i^\top \bar{\mathbf{M}}_i \mathbf{K}_i \ddot{\boldsymbol{p}}_i = \mathbf{J}_i^\top \bar{\boldsymbol{f}}_i - \mathbf{J}_i^\top \boldsymbol{\mu}_i = \mathbf{J}_i^\top \bar{\boldsymbol{f}}_i$$

see (11) and (12). If $\bar{\mathbf{M}}_i \in \mathbb{R}^{d\times d}$ is symmetric, positive definite then the coefficient $\mathbf{J}_i^\top \bar{\mathbf{M}}_i \mathbf{J}_i \in \mathbb{R}^{n_i \times n_i}$ of the joint accelerations $\ddot{\boldsymbol{q}}_i$ in (14) is symmetric, positive definite as well and (14) may be solved w.r.t. $\ddot{\boldsymbol{q}}_i$:

$$\ddot{\boldsymbol{q}}_i = -(\mathbf{J}_i^\top \bar{\mathbf{M}}_i \mathbf{J}_i)^{-1} (\mathbf{J}_i^\top \bar{\mathbf{M}}_i (\mathbf{H}_i \ddot{\boldsymbol{p}}_{\pi_i} + \boldsymbol{k}_i^{(II)}) + \mathbf{J}_i^\top \bar{\boldsymbol{f}}_i \quad (15)$$

Inserting this expression in (9) we get

$$\ddot{\boldsymbol{p}}_i = -\bar{\mathbf{H}}_i \ddot{\boldsymbol{p}}_{\pi_i} - \bar{\boldsymbol{k}}_i^{(II)} \quad (16)$$

with

$$\bar{\mathbf{H}}_i := \mathbf{K}_i^{-1} (\mathbf{I}_d - \mathbf{J}_i (\mathbf{J}_i^\top \bar{\mathbf{M}}_i \mathbf{J}_i)^{-1} \mathbf{J}_i^\top \bar{\mathbf{M}}_i)\, \mathbf{H}_i, \quad (17a)$$

$$\bar{\boldsymbol{k}}_i^{(II)} := \mathbf{K}_i^{-1} (\mathbf{I}_d - \mathbf{J}_i (\mathbf{J}_i^\top \bar{\mathbf{M}}_i \mathbf{J}_i)^{-1} \mathbf{J}_i^\top \bar{\mathbf{M}}_i)\, \boldsymbol{k}_i^{(II)} - \mathbf{K}_i^{-1} \mathbf{J}_i (\mathbf{J}_i^\top \bar{\mathbf{M}}_i \mathbf{J}_i)^{-1} \mathbf{J}_i^\top \bar{\boldsymbol{f}}_i) \quad (17b)$$

Eq. (16) is used to evaluate all (absolute) accelerations $\ddot{\boldsymbol{p}}_i, (i = 1, \ldots, N)$, recursively beginning at the root body. For the multibody system model in Fig. 3, this *second forward* recursion starts again at body $(\bullet)^{(1)}$ and takes into account that $\ddot{\boldsymbol{p}}_{\pi_1} = \ddot{\boldsymbol{p}}_0 = \mathbf{0}$ since the root body is inertially fixed. The absolute acceleration $\ddot{\boldsymbol{p}}_1 = -\bar{\boldsymbol{k}}_i^{(II)}$ is obtained from (16) with $i = 1$ and may be used in the next step to get the absolute accelerations of body $(\bullet)^{(2)}$ since $\ddot{\boldsymbol{p}}_{\pi_2} = \ddot{\boldsymbol{p}}_1$. The forward recursion proceeds with $\ddot{\boldsymbol{p}}_3$ in the left branch of the multibody system model and with $\ddot{\boldsymbol{p}}_4$, $\ddot{\boldsymbol{p}}_5$ in its right branch, see Fig. 3. Finally, all joint accelerations $\ddot{\boldsymbol{q}}_i, (i = 1, \ldots, N)$, are obtained from (15). In time integration, the current function values of $\ddot{\boldsymbol{q}}_i(t)$ may be used to evaluate the right hand side of the equations of motion in any ODE time integration method.

4 The rank deficient case

(Very) small masses or (nearly) singular inertia tensors in a multibody system model may be interpreted as small perturbations. The analysis of Section 2.1 suggests to study a reduced system that neglects these perturbations. Therefore, we consider now the limit case of multibody systems that have one or more bodies with zero mass or singular inertia tensor, i.e., with a rank-deficient body mass matrix $\mathbf{M}_i$. In that case, the classical recursive multibody formalism of Section 3 may fail since it is based on the inverse $(\mathbf{J}_i^\top \bar{\mathbf{M}}_i \mathbf{J}_i)^{-1}$ of projected body mass matrices.

Eq. (14) allows to characterize the rank deficient case more precisely. As long as all projected mass matrices $\mathbf{J}_i^\top \bar{\mathbf{M}}_i \mathbf{J}_i \in \mathbb{R}^{n_i \times n_i}$ with joint Jacobians $\mathbf{J}_i$ and appropriately defined condensed body mass matrices $\bar{\mathbf{M}}_i$ are non-singular, the classical recursive multibody formalism of Section 3 may be applied without any modifcations. In the rank deficient case, however, we have $r_i := \operatorname{rank}(\mathbf{J}_i^\top \bar{\mathbf{M}}_i \mathbf{J}_i) < n_i$ and (14) can not be solved uniquely w.r.t. the joint accelerations $\ddot{\boldsymbol{q}}_i$.

In that case, the n_i differential equations (14) may be decoupled into r_i second order differential equations depending on $\ddot{\boldsymbol{q}}_i$ and another set of $n_i - r_i$ equations that are independent of all joint accelerations $\ddot{\boldsymbol{q}}$. With appropriate damping terms in the multibody system model, see Section 2.2 and [1], these $n_i - r_i$ equations define an implicit system of $n_i - r_i$ first order differential equations for the generalized coordinates $\boldsymbol{q}_i^{(t)}$. To separate second and first order differential equations, Eq. (14) is multiplied from the left by $(\mathbf{J}_i^\top \bar{\mathbf{M}}_i \mathbf{J}_i)^+$:

$$(\mathbf{J}_i^\top \bar{\mathbf{M}}_i \mathbf{J}_i)^+ (\mathbf{J}_i^\top \bar{\mathbf{M}}_i \mathbf{J}_i)\, \ddot{\boldsymbol{q}}_i = -(\mathbf{J}_i^\top \bar{\mathbf{M}}_i \mathbf{J}_i)^+ (\mathbf{J}_i^\top \bar{\mathbf{M}}_i (\mathbf{H}_i \ddot{\boldsymbol{p}}_{\pi i} + \boldsymbol{k}_i^{(II)}) + \mathbf{J}_i^\top \bar{\boldsymbol{f}}_i). \quad (18)$$

Here, $\mathbf{A}^+ \in \mathbb{R}^{n\times m}$ denotes the Moore-Penrose pseudo-inverse of a given matrix $\mathbf{A} \in \mathbb{R}^{m\times n}$, see [5]. This pseudo-inverse $\mathbf{A}^+$ maps any given vector $\boldsymbol{b} \in \mathbb{R}^m$ to the minimum norm solution $\boldsymbol{x} = \mathbf{A}^+\boldsymbol{b} \in \mathbb{R}^n$ of the least squares problem $\|\boldsymbol{b} - \mathbf{A}\boldsymbol{x}\|_2 \to \min$, i.e.,

$$\boldsymbol{x} = \mathbf{A}^+ \boldsymbol{b} \;\Leftrightarrow\; \begin{cases} \|\boldsymbol{b} - \mathbf{A}\boldsymbol{x}\|_2 = \min\{\|\boldsymbol{b} - \mathbf{A}\tilde{\boldsymbol{\xi}}\|_2 : \tilde{\boldsymbol{\xi}} \in \mathbb{R}^n\}, \\ \|\boldsymbol{b} - \mathbf{A}\boldsymbol{\xi}\|_2 = \min\{\|\boldsymbol{b} - \mathbf{A}\tilde{\boldsymbol{\xi}}\|_2 : \tilde{\boldsymbol{\xi}} \in \mathbb{R}^n\} \end{cases}$$

$$\Rightarrow \|\boldsymbol{\xi}\|_2 \geq \|\boldsymbol{x}\|_2 .$$

For non-singular matrices $\mathbf{A} \in \mathbb{R}^{n\times n}$, the Moore-Penrose pseudo-inverse $\mathbf{A}^+$ coincides with the classical inverse matrix $\mathbf{A}^{-1}$ since $\boldsymbol{x} = \mathbf{A}^{-1}\boldsymbol{b}$ is the unique vector with $\|\boldsymbol{b} - \mathbf{A}\boldsymbol{x}\|_2 = \|\boldsymbol{b} - \mathbf{A}\mathbf{A}^{-1}\boldsymbol{b}\|_2 = 0$ and $\|\boldsymbol{b} - \mathbf{A}\tilde{\boldsymbol{\xi}}\|_2 > 0, (\tilde{\boldsymbol{\xi}} \in \mathbb{R}^n \setminus \{\mathbf{A}^{-1}\boldsymbol{b}\})$.

In that case, we have in (14) a full rank matrix $\mathbf{J}_i^\top \bar{\mathbf{M}}_i \mathbf{J}_i \in \mathbb{R}^{n_i \times n_i}$, i.e., $r_i = n_i$, and (18) simplifes to the explicit expression

$$\ddot{\boldsymbol{q}}_i = -(\mathbf{J}_i^\top \bar{\mathbf{M}}_i \mathbf{J}_i)^+ (\mathbf{J}_i^\top \bar{\mathbf{M}}_i (\mathbf{H}_i \ddot{\boldsymbol{p}}_{\pi_i} + \boldsymbol{k}_i^{(II)}) + \mathbf{J}_i^\top \bar{\boldsymbol{f}}_i). \quad (19)$$

since $(\mathbf{J}_i^\top \bar{\mathbf{M}}_i \mathbf{J}_i)^+ (\mathbf{J}_i^\top \bar{\mathbf{M}}_i \mathbf{J}_i) \ddot{\boldsymbol{q}}_i = (\mathbf{J}_i^\top \bar{\mathbf{M}}_i \mathbf{J}_i)^{-1} (\mathbf{J}_i^\top \bar{\mathbf{M}}_i \mathbf{J}_i) \ddot{\boldsymbol{q}}_i = \ddot{\boldsymbol{q}}_i$, see also (15).

In the rank deficient case, we have $r_i < n_i$ and use an orthogonal set of n_i linearly independent normalized eigenvectors $\boldsymbol{x}_i^{(l)} \in \mathbb{R}^{n_i}, (l = 1, \ldots, n_i)$, of matrix $\mathbf{J}_i^\top \bar{\mathbf{M}}_i \mathbf{J}_i$ to define an orthogonal transformation matrix $\mathbf{X}_i = [\boldsymbol{x}_i^{(1)}, \ldots, \boldsymbol{x}_i^{(n_i)}] \in \mathbb{R}^{n_i \times n_i}$:

$$(\mathbf{J}_i^\top \bar{\mathbf{M}}_i \mathbf{J}_i) \mathbf{X}_i = \mathbf{X}_i \boldsymbol{\Lambda}_i$$

with a diagonal matrix $\boldsymbol{\Lambda}_i$ containing the eigenvalues of $\mathbf{J}_i^\top \bar{\mathbf{M}}_i \mathbf{J}_i$ on the main diagonal. Arranging the

column vectors of $\mathbf{X}_i$ such that the last $n_i - r_i$ columns correspond to the zero eigenvalues of $\mathbf{J}_i^\top \bar{\mathbf{M}}_i \mathbf{J}_i$, we get

$$(\mathbf{J}_i^\top \bar{\mathbf{M}}_i \mathbf{J}_i)^+ (\mathbf{J}_i^\top \bar{\mathbf{M}}_i \mathbf{J}_i) = \mathbf{X}_i \begin{pmatrix} \mathbf{I}_{r_i} & \mathbf{0} \\ \mathbf{0} & \mathbf{0} \end{pmatrix} \mathbf{X}_i^\top$$

and (18) defines the system of r_i second order differential equations

$$(\mathbf{I}_{r_i}\ \mathbf{0})\mathbf{X}_i^\top \ddot{\boldsymbol{q}}_i = -(\mathbf{I}_{r_i}\ \mathbf{0})\mathbf{X}_i^\top (\mathbf{J}_i^\top \bar{\mathbf{M}}_i \mathbf{J}_i)^+ (\mathbf{J}_i^\top \bar{\mathbf{M}}_i (\mathbf{H}_i \ddot{\boldsymbol{p}}_{\pi_i} + \boldsymbol{k}_i^{(II)}) + \mathbf{J}_i^\top \bar{\boldsymbol{f}}_i). \quad (20a)$$

Substituting $\mathbf{J}_i^\top \bar{\mathbf{M}}_i \mathbf{J}_i$ in (14) by $\mathbf{X}_i \boldsymbol{\Lambda}_i \mathbf{X}_i^\top$ and multiplying the resulting equations from the left by $-(\mathbf{0}\ \mathbf{I}_{n_i - r_i})\mathbf{X}_i^\top$, we get an additional system of $n_i - r_i$ differential equations being independent of $\ddot{\boldsymbol{q}}_i$ that gets the form

$$(\mathbf{0}\ \mathbf{I}_{n_i - r_i})\mathbf{X}_i^\top \mathbf{J}_i^\top \bar{\boldsymbol{f}}_i \quad (20b)$$

since $(\mathbf{0}\ \mathbf{I}_{n_i - r_i})\mathbf{X}_i^\top \mathbf{J}_i^\top \bar{\boldsymbol{M}}_i = \mathbf{0}$, see [1]. Note, that the right hand side of (20b) may depend on t, $\boldsymbol{q}(t)$ and $\dot{\boldsymbol{q}}(t)$.

Up to now, we did not specify how to define the condensed body mass matrix $\bar{\mathbf{M}}_i$ and the condensed force vector $\bar{\boldsymbol{f}}_i$ in (13) in the case of a rank deficient projected mass matrix $\mathbf{J}_i^\top \bar{\mathbf{M}}_i \mathbf{J}_i$ for a successor body $(\bullet)^{(i)}$, i.e., for a body $(\bullet)^{(i)}$ with $\pi_j = i$, $j \in I_i$. As in (18), it seems to be natural to substitute the classical inverse $(\mathbf{J}_j^\top \bar{\mathbf{M}}_j \mathbf{J}_j)^{-1}$ in the right hand sides of (13) by its Moore-Penrose counterpart $(\mathbf{J}_j^\top \bar{\mathbf{M}}_j \mathbf{J}_j)^+$. In the full rank case ($r_i = n_i$), classical inverse and Moore-Penrose pseudo-inverse coincide anyway. In the rank deficient case ($r_i < n_i$), we observe that the Moore-Penrose axioms $\mathbf{A}\mathbf{A}^+\mathbf{A} = \mathbf{A}$ and $\mathbf{A}^+\mathbf{A}\mathbf{A}^+ = \mathbf{A}^+$, see [5], imply

$$\bar{\mathbf{M}}_j \mathbf{J}_j (\mathbf{I}_{n_j} - (\mathbf{J}_j^\top \bar{\mathbf{M}}_j \mathbf{J}_j)^+ (\mathbf{J}_j^\top \bar{\mathbf{M}}_j \mathbf{J}_j)) = \mathbf{0}_{d \times n_j}, \quad (21a)$$

$$(\mathbf{I}_{n_j} - (\mathbf{J}_j^\top \bar{\mathbf{M}}_j \mathbf{J}_j)(\mathbf{J}_j^\top \bar{\mathbf{M}}_j \mathbf{J}_j)^+) \mathbf{J}_j^\top \bar{\mathbf{M}}_j = \mathbf{0}_{n_j \times d}, \quad (21b)$$

see [1, Appendix A]. These properties of the Moore-Penrose pseudo-inverse allow to prove that (12) remains valid in the rank deficient case if the inverse matrices $(\mathbf{J}_j^\top \bar{\mathbf{M}}_j \mathbf{J}_j)^{-1}$ in the right hand sides of (13) are systematically substituted by $(\mathbf{J}_j^\top \bar{\mathbf{M}}_j \mathbf{J}_j)^+$, see [1] for a more detailed discussion. Therefore, the condensed body mass matrices $\bar{\mathbf{M}}_i$ and the condensed force vectors $\bar{\boldsymbol{f}}_i$ may again be obtained by a backward recursion starting at the leaf bodies ($I_i = \emptyset$) and proceeding down to the root.

To evaluate the absolute accelerations $\ddot{\boldsymbol{p}}_i$ by forward recursion, we substitute also in the defnition of $\bar{\mathbf{H}}_i$ and $\bar{\boldsymbol{k}}_i^{(II)}$, see (17), the classical inverse by the Moore Penrose pseudo-inverse, i.e., $(\mathbf{J}_i^\top \bar{\mathbf{M}}_i \mathbf{J}_i)^{-1}$ by $(\mathbf{J}_i^\top \bar{\mathbf{M}}_i \mathbf{J}_i)^+$. Then, Eq. (16) gets the general form

$$\ddot{\boldsymbol{p}}_i = -\bar{\mathbf{H}}_i \ddot{\boldsymbol{p}}_{\pi_i} - \bar{\boldsymbol{k}}_i^{(II)} - \mathbf{K}_i^{-1} \mathbf{J}_i (\mathbf{I}_{n_i} - (\mathbf{J}_i^\top \bar{\mathbf{M}}_i \mathbf{J}_i)^+ (\mathbf{J}_i^\top \bar{\mathbf{M}}_i \mathbf{J}_i)) \ddot{\boldsymbol{q}}_i \quad (22)$$

which is in the rank-deficient case substantially more complex than for non-singular matrices $\mathbf{J}_i^\top \bar{\mathbf{M}}_i \mathbf{J}_i$. The additional term $(\mathbf{I}_{n_i} - (\mathbf{J}_i^\top \bar{\mathbf{M}}_i \mathbf{J}_i)^+ (\mathbf{J}_i^\top \bar{\mathbf{M}}_i \mathbf{J}_i))\ \ddot{\boldsymbol{q}}_i$ in the right hand side of (22) can not be obtained by pure linear transformations since it simply does not appear in the projected equations of motion (18).

It is an important (and non-trivial) observation that this additional term does not affect the successors of body $(\bullet)^{(i)}$ in the kinematic tree (if there are any). Suppose $I_i \neq \emptyset$ and consider a (direct) successor $(\bullet)^{(j)}$ of body $(\bullet)^{(i)}$, $\pi_j = i$. The key to a forward recursion algorithm in the case of rank deficient projected body mass matrices $\mathbf{J}_i^\top \bar{\mathbf{M}}_i \mathbf{J}_i$ is the observation that defnition (13a) with $(\mathbf{J}_i^\top \bar{\mathbf{M}}_i \mathbf{J}_i)^{-1}$ being substituted by $(\mathbf{J}_i^\top \bar{\mathbf{M}}_i \mathbf{J}_i)^+$ implies

$$\bar{\mathbf{M}}_j \mathbf{K}_j \bar{\mathbf{H}}_j \mathbf{K}_i^{-1} \mathbf{J}_i (\mathbf{I}_{n_i} - (\mathbf{J}_i^\top \bar{\mathbf{M}}_i \mathbf{J}_i)^+ (\mathbf{J}_i^\top \bar{\mathbf{M}}_i \mathbf{J}_i)) = \mathbf{0}_{d \times n_i}$$

and

$$\mathbf{0} = \bar{\mathbf{M}}_j \mathbf{K}_j (\ddot{\boldsymbol{p}}_j - \bar{\mathbf{H}}_j \bar{\mathbf{H}}_i \ddot{\boldsymbol{p}}_{\pi_i} - \bar{\mathbf{H}}_j \bar{\boldsymbol{k}}_i^{(II)} + \bar{\boldsymbol{k}}_j^{(II)}), \quad (23)$$

see [1]. It is reasonable to assume that the bodies with rank-deficient body mass matrix $\mathbf{M}_i$ are isolated in the kinematic tree, i.e., the predecessor of a body $(\bullet)^{(i)}$ with rank-deficient $\mathbf{M}_i$ is either the root body ($\pi_i = 0$) or a body with non-singular body mass matrix:

$$\text{rank } \mathbf{M}_i < d \Rightarrow (\pi_i = 0 \text{ or rank } \mathbf{M}_{\pi_i} = d). \quad (24)$$

This technical assumption allows to evaluate $\ddot{\boldsymbol{p}}_j$ for all successors $(\bullet)^{(j)}$ of a body $(\bullet)^{(i)}$ with rank deficient body mass matrix $\mathbf{M}_i$ since rank $\mathbf{M}_i < d$, $\pi_i = i$ and (24) imply that the condensed body mass matrix $\bar{\mathbf{M}}_j$ in (23) is non-singular and

$$\ddot{\boldsymbol{p}}_j = \bar{\mathbf{H}}_j \bar{\mathbf{H}}_i \ddot{\boldsymbol{p}}_{\pi_i} + \bar{\mathbf{H}}_j \bar{\boldsymbol{k}}_i^{(II)} - \bar{\boldsymbol{k}}_j^{(II)}. \quad (25)$$

As a practical consequence, bodies $(\bullet)^{(i)}$ with rank deficient projected body mass matrix $\mathbf{J}_i^\top \bar{\mathbf{M}}_i \mathbf{J}_i$ are skipped in the forward recursion and the absolute accelerations $\ddot{\boldsymbol{p}}_j$ of all successor bodies $(\bullet)^{(j)}$,$(\pi_j = i)$, are computed by (25). The corresponding equations of motion for $\ddot{\boldsymbol{q}}_j$ contain $(\mathbf{I}_{n_i} - (\mathbf{J}_i^\top \bar{\mathbf{M}}_i \mathbf{J}_i)^+ (\mathbf{J}_i^\top \bar{\mathbf{M}}_i \mathbf{J}_i))\ \ddot{\boldsymbol{q}}_i$ as well, see [1]:

$$\ddot{\boldsymbol{q}}_j - (\mathbf{J}_j^\top \bar{\mathbf{M}}_j \mathbf{J}_j)^+ \mathbf{J}_j^\top \bar{\mathbf{M}}_j \mathbf{H}_j \mathbf{K}_i^{-1} \mathbf{J}_i (\mathbf{I}_{n_i} - (\mathbf{J}_i^\top \bar{\mathbf{M}}_i \mathbf{J}_i)^+ (\mathbf{J}_i^\top \bar{\mathbf{M}}_i \mathbf{J}_i))\ \ddot{\boldsymbol{q}}_i = (\mathbf{J}_j^\top \bar{\mathbf{M}}_j \mathbf{J}_j)^+ (\mathbf{J}_j^\top \bar{\mathbf{M}}_j (\mathbf{H}_j \bar{\mathbf{H}}_i \ddot{\boldsymbol{p}}_{\pi_i} + \bar{\mathbf{H}}_j \bar{\boldsymbol{k}}_i^{(II)} - \boldsymbol{k}_j^{(II)}) - \mathbf{J}_j^\top \bar{\boldsymbol{f}}_j). \quad (26)$$

In the full rank case, the classical update formula (16) for $\ddot{\boldsymbol{p}}_i$ may be used instead since the additional term $(\mathbf{I}_{n_i} - (\mathbf{J}_i^\top \bar{\mathbf{M}}_i \mathbf{J}_i)^+ (\mathbf{J}_i^\top \bar{\mathbf{M}}_i \mathbf{J}_i))\ \ddot{\boldsymbol{q}}_i$ in the right hand side of (22) vanishes identically. The corresponding equations of motion for bodies $(\bullet)^{(j)}$ with $\pi_j = i$ are given in (19) and (20), respectively.

To illustrate the modifed forward recursion we consider again the tree structured system in Fig. 3 and suppose that the projected

body mass matrix of body $(\bullet)^{(2)}$ is rank deficient, $r_2 := \text{rank } \mathbf{J}_2^\top \bar{\mathbf{M}}_2 \mathbf{J}_2 < n_2$, and all other projected body mass matrices are non-singular. As in the classical case, the second forward recursion starts at the root body and evaluates $\ddot{\boldsymbol{p}}_1$ according to (16) with $i = 1$.
Then, body $(\bullet)^{(2)}$ has to be skipped since $r_2 < n_2$. The absolute accelerations $\ddot{\boldsymbol{p}}_3$ and $\ddot{\boldsymbol{p}}_4$ of bodies $(\bullet)^{(3)}$ and $(\bullet)^{(4)}$ are computed from (25) with $i = 2$, $\pi_i = 1$ and $j = 3$ and $j = 4$, respectively. Finally, $\ddot{\boldsymbol{p}}_5$ may be obtained from (16) with $i = 5$.
The resulting equations of motion are given by (19) with $i = 1$, $\pi_i = 0$ and $\ddot{\boldsymbol{p}}_{\pi_i} = \mathbf{0}$, by (20) with $i = 2$, $\pi_i = 1$, by (26) with $j = 3$, $i = \pi_i = 2$, $\pi_i = 1$, by (26) with $j = 4$, $i = \pi_i = 2$, $\pi_i = 1$ and by (19) with $i = 5$, $\pi_i = 4$. They do not contain the "missing" absolute accelerations $\ddot{\boldsymbol{p}}_2$ of the body with rank-deficient projected body mass matrix ($r_2 < n_2$).

5 Conclusions

Motivated by results from singular perturbation theory, multibody system models with bodies of small mass or nearly singular inertia terms are analysed considering the limit case of systems with rank-deficient body mass matrices. Replacing in a classical recursive multibody formalism the inverse of projected body mass matrices by their Moore-Penrose pseudo-inverse, the algorithm may be adapted to the rankdeficient case.
For each body with rank-deficient projected body mass matrix, a mixed system of first and second order differential equations is obtained if there are appropriate damping terms in the force elements acting at this "zero mass" body. Further investigations will be necessary to analyse practical aspects of this regularity assumption in more detail and to extend the modifed recursive formalism from rigid to fexible multibody systems.

Acknowledgements

This research on singularly perturbed multibody system models was funded by the German Federal Ministry of Education and Research within the programme "Mathematics for Innovation in Industry and Services" (BMBF grant 05M10NHB).

References

[1] M. Arnold. A recursive multibody formalism for systems with small mass and inertia terms. Mech. Sci., 4:221 231, 2013.

[2] B. Burgermeister, M. Arnold, and A. Eichberger. Smooth velocity approximation for constrained systems in real-time simulation. Multibody System Dynamics, 26:1 14, 2011.

[3] E. Eich-Soellner and C. Führer. Numerical Methods in Multibody Dynamics. Teubner Verlag, Stuttgart, 1998.

[4] A. Eichberger and W. Rulka. Process save reduction by macro joint approach: The key to real time and efficient vehicle simulation. Vehicle System Dynamics, 41:401 413, 2004.

[5] G.H. Golub and C.F. van Loan. Matrix Computations. The Johns Hopkins University Press, Baltimore London, 3rd edition, 1996.

[6] T. Gorius, R. Seifried, and P. Eberhard. Approximate feedforward control of fexible multibody systems. In J.B. Jonker et al. (eds.), Program and abstracts of the EUROMECH Colloquium 524, pages 22 23. University of Twente, 2012.

[7] C. Hager and B. Wohlmuth. Analysis of a space-time discretization for dynamic elasticity problems based on mass-free surface elements. SIAM J. Numer. Anal., 47:1863 1885, 2009.

[8] E. Hairer and G. Wanner. Solving Ordinary Differential Equations. II. Stiff and Differential Alrebraic Problems. Springer, Berlin, 2nd ed., 1996.

[9] C. Lubich. Integration of stiff mechanical systems by Runge-Kutta methods.
Z. Angew. Math. Phys., 44:1022 1053, 1993.

[10] C. Lubich, U. Nowak, U. Pöhle, and C. Engstler. MEXX-Numerical software for the integration of constrained mechanical multibody systems. Technical Report SC 92 12, ZIB Berlin, 1992.

[11] K. Nipp. Smooth attractive invariant manifolds of singularly perturbed ODE's. Technical Report 92-13, SAM, ETH Zürich, 1992.

[12] W. Schiehlen. Multibody system dynamics: roots and perspectives. Multibody System Dynamics, 1:149 188, 1997.

[13] R. Schönen. Strukturdynamische Mehrkörpersimulation des Verbrennungsmotors mit elastohydrodynamischer Grundlagerkopplung. Fortschrittsberichte Strukturanalyse und Tribologie, Band 15. Kassel University Press, 2003.

[14] T. Stumpp. Asymptotic expansions and attractive invariant manifolds of strongly damped mechanical systems. ZAMM, 88:630 643, 2008.

[15] S. Weber, M. Arnold, and M. Valasek. Quasistatic approximations for stiff second-order differential equations. Appl. Num. Math., 62:1579 1590, 2012.

Topology optimization in flexible multibody dynamics

A. Held und R. Seifried
Institute of Engineering and Computational Mechanics, University of Stuttgart

Abstract

Lightweight techniques are applied increasingly often for machine designs in order to reduce the moving masses and, thus, the energy consumption. However, as a result the stiffness of the system decreases causing undesired deformation which deteriorate the system performance. In order to facilitate the early design process of lightweight machines, topology optimization can be employed. Thereby, to capture the system behavior and the machine loads as precisely as possible, the optimization has to be performed by means of simulation models which use the method of flexible multibody systems. In this work, a topology optimization procedure applying the Solid Isotropic Material with Penalization (SIMP) approach is presented and demonstrated using the example of a flexible two-arm manipulator. The deformations of the two flexible arms are assumed to be small and, thus, the floating frame of reference formulation is used.

1 Introduction

Energy effciency is a crucial issue in modern machine design and in many robotic applications. Examples are service robots or medical manipulators as well as traditional industrial robots and machine tools operating at high speeds. In order to achieve low energy consumption, the use of lightweight structural designs is necessary. However, as a result the stiffness of the system decreases and undesired elastic deformations occur which deteriorate the performance of the system. For example, in lightweight manipulators structural flexibility might lead to large unacceptable end-effector tracking errors. In order to achieve good system performance, the actual dynamic loads must be taken into account in the design of the system's components, either based on equivalent static loads, see Albers et al [2007]; Kang and Park [2005] or using an integrated dynamic approach, see Brüls [2011]. In this work, a topology optimization procedure for lightweight machine designs is presented to improve the dynamical behavior of flexible multibody systems. In order to capture both the large nonlinear working motion and the deformation of the bodies in the simulation, the system is modeled as flexible multibody system, using the floating frame of reference formulation. In this approach, the global nonlinear working motion is described by a reference frame while the elastic deformations are described with respect to the reference frame using global shape functions. The global shape functions are commonly obtained from finite element models of the elastic bodies by model reduction, see Lehner [2007]. Structural optimizations are often performed using finite element models. Thereby the objective functions are usually defined with respect to compliance, displacements or stresses of the structure obtained from a set of static load cases. In contrast, the objective functions are in this work computed from fully dynamical simulations. Thus, all relevant loads on the flexible members of the system are captured. Consequently, all steps including the finite element modeling, the model reduction, the derivation of the equations of motion and the transient simulation have to be performed in each optimization loop. The procedure is presented using the example of a flexible 2-arm manipulator. For the topology optimization the SIMP approach, see Bendsøe and Sigmund [2003], is employed to distribute a limited amount of mass in a reference domain. It is shown, that topology optimization is applicable to efficiently design flexible multibody systems such as lightweight manipulators and improve their dynamical behavior.

2 Flexible multibody systems

Flexible multibody systems are an extension of classical rigid multibody systems, where in addition to the large nonlinear rigid body motions also some of the bodies show non negligible deformations. Restricting the deformations to be small, as occurring in most typical machine dynamics applications, flexible bodies can be incorporated effciently in multibody systems using the floating frame of reference approach. This approach is described in detail in Shabana [2005]; Schwertassek and Wallrapp [1999]. Here, only a brief summary of the main ideas shall be given. Using the floating frame of reference, the deformation of a flexible body is described in a reference frame K_R which experience large translational and rotational motion, see

Fig. 1. For example, the absolute position vector $\boldsymbol{r}_{IP}$ of a point P of the elastic body is expressed as

$$\boldsymbol{r}_{IP} = \boldsymbol{r}_{IR} + \boldsymbol{r}_{\mathrm{RP}} = \boldsymbol{r}_{IR} + \boldsymbol{R}_{RP} + \boldsymbol{u}_P\,, \quad (1)$$

which is composed of the large nonlinear motion of the frame of reference $\boldsymbol{r}_{IR}$ and the relative position of the point $\boldsymbol{r}_{RP}$. The latter is composed of the relative position in reference configuration $\boldsymbol{R}_{RP}$ and the elastic displacement $\boldsymbol{u}_P$. The small elastic displacements are expressed in this floating frame of reference and are approximated using a global Ritz-approach to separate the time- and position-dependent parts,

$$\boldsymbol{u}_P\,(\boldsymbol{R}_{RP}\,,t) \approx \boldsymbol{\Phi}(\boldsymbol{R}_{RP})\boldsymbol{q}_e(t). \quad (2)$$

Thereby $\boldsymbol{q}_e$ are the elastic generalized coordinates and the matrix $\boldsymbol{\Phi}$ contains the shape functions. For the rotations, a similar Ritz-approach with the corresponding shape functions $\boldsymbol{\Psi}$ is used. The shape functions can be computed from a structural analysis of the elastic body, e.g. by a finite element modal analysis, and are provided by Standard Input Data (SID) files, see Wallrapp [1994]. During the modeling the type of floating frame of reference for the flexible body must be chosen. In this work the frame of reference is attached to one node of the body, resulting in a tangent orientation of the reference frame with respect to the deformed body, which is also called a tangent frame. The tangent frames are here located in the joints of the system.

For systems without kinematic loops the equations of motion in minimal form are obtained by considering all constraints in the assembled system depending on generalized coordinates $\boldsymbol{q} = [\boldsymbol{q}_{\mathrm{r}}^{\mathrm{T}}\,, \boldsymbol{q}_{\mathrm{e}}^{\mathrm{T}}]^{\mathrm{T}} \in \mathbb{R}^f$. Thereby, the vector of generalized coordinates contains the coordinates $\boldsymbol{q}_r \in \mathbb{R}^{f_r}$ representing the f_r degrees of freedom of the rigid body motion and the elastic coordinates $\boldsymbol{q}_e \in \mathbb{R}^{f_e}$. These are now the collection of the elastic generalized coordinates of all flexible bodies. The equations of motion in minimal coordinates are displayed as

$$\boldsymbol{M}(\boldsymbol{q})\ddot{\boldsymbol{q}} + \boldsymbol{k}(\boldsymbol{q},\,\dot{\boldsymbol{q}}) + \tilde{\boldsymbol{k}}(\boldsymbol{q},\,\dot{\boldsymbol{q}}) = \boldsymbol{g}(\boldsymbol{q},\,\dot{\boldsymbol{q}}) + \boldsymbol{B}(\boldsymbol{q})\boldsymbol{u}, \quad (3)$$

where $\boldsymbol{M} \in \mathbb{R}^{f\times f}$ is the generalized mass matrix, $\boldsymbol{k} \in \mathbb{R}^f$ the vector of Coriolis, gyroscopic and centrifugal forces, $\tilde{\boldsymbol{k}} \in \mathbb{R}^f$ the vector of inner forces, and $\boldsymbol{g} \in \mathbb{R}^f$ the vector of generalized applied forces. The input matrix $\boldsymbol{B} \in \mathbb{R}^{f\times m}$ distributes the control inputs $\boldsymbol{u} \in \mathbb{R}^m$ onto the directions of the generalized coordinates. Following the partitioning of the generalized coordinates into rigid and elastic coordinates, the equations of motion can also be displayed as

$$\begin{bmatrix} \boldsymbol{M}_{rr} & \boldsymbol{M}_{re} \\ \boldsymbol{M}_{re}^T & \boldsymbol{M}_{ee} \end{bmatrix} \begin{bmatrix} \ddot{\boldsymbol{q}}_r \\ \ddot{\boldsymbol{q}}_e \end{bmatrix} + \begin{bmatrix} \boldsymbol{k}_r \\ \boldsymbol{k}_e \end{bmatrix} + \begin{bmatrix} 0 \\ \boldsymbol{K}_e\boldsymbol{q} + \boldsymbol{D}_e\dot{\boldsymbol{q}} \end{bmatrix} = \begin{bmatrix} \boldsymbol{g}_r \\ \boldsymbol{g}_e \end{bmatrix} + \begin{bmatrix} \boldsymbol{u} \\ 0 \end{bmatrix}. \quad (4)$$

Here $\boldsymbol{K}_e$ and $\boldsymbol{D}_e$ are the structural stiffness and damping matrix. In the considered flexible multibody systems the actuation occurs only at the joints of the systems. Since a tangent frame of reference is used for the elastic bodies, the control inputs $\boldsymbol{u}$ act only on the rigid coordinates $\boldsymbol{q}_r$. In order to obtain a good performance in tracking the end-effector trajectories, an efficient feed-forward control supplemented by an additional feedback control is often necessary.

A simple feed-forward control strategy is inverse dynamics, also known as computed torque, see Spong, Hutchinson and Vidyasagar [2006]. Thereby, in the control design the elastic deformations are neglected. At first, using inverse kinematic of an equivalent rigid system, the desired trajectories $\boldsymbol{q}_{r,d}$ of the rigid generalized coordinates, also called joint coordinates, are computed from the desired end-effector trajectory $\boldsymbol{r}_{\mathrm{d}}^{\mathrm{ef}}$. Then, the control inputs $\boldsymbol{u}_d$ for the rigid body subsystem are calculated from the rigid part of the equations of motion as

$$\boldsymbol{u}_d = \boldsymbol{M}_{rr}(\boldsymbol{q}_{r,d})\ddot{\boldsymbol{q}}_{r,d} + \boldsymbol{k}_r(\boldsymbol{q}_{r,d}, \dot{\boldsymbol{q}}_{r,d}) - \boldsymbol{g}_r(\boldsymbol{q}_{r,d}, \dot{\boldsymbol{q}}_{r,d}), \quad \text{with} \quad \boldsymbol{q}_e = 0. \quad (5)$$

Other more advanced tracking control approaches are based on nonlinear control theory, see e.g.

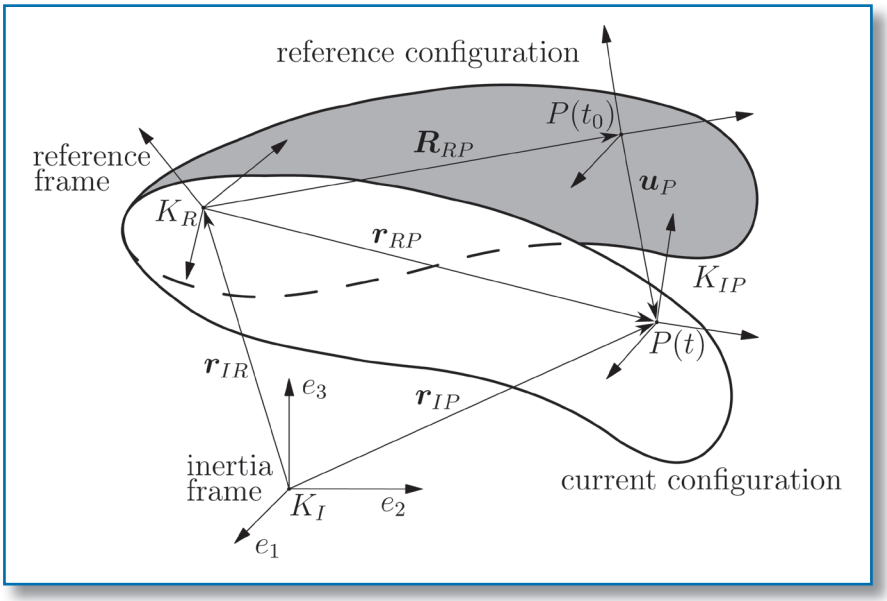

Figure 1:
Kinematic of a flexible body using the floating frame of reference approach.

Seifried, Held and Dietmann [2011]. They provide often a much more accurate feed-forward control, but their design is much more complex. In Seifried and Held [2011] it is shown, that an optimized structural design as aspired in this paper can be combined with such advanced control approaches. Thus, by this combination tracking errors can be effciently further reduced. In this work, the focus is on the influence of the flexibilities on the system performance. The influence of the control strategy and parameters shall be neglected. Therefore, the positions, velocities and accelerations of the rigid generalized coordinates $\boldsymbol{q}_r$ are defined by rheonomic constraints. The approach resembles an inverse dynamics feed-forward control combined with an ideal feedback control. However, no control parameters must be identified and objective functions are free from control influences.

3 Application example

The optimization procedure presented in this paper is applied to a serial flexible manipulator, which is shown schematically in Fig. 2(a). The system moves in the e_1e_2-plane and consists of a rigid carriage with one translational degree of freedom s and two flexible arms, which are connected by revolute joints. The rigid body motions are described by the coordinates $\boldsymbol{q}_r = [s, \alpha, \beta]$. At the end of the first and of the second arm, bodies are added to capture the inertia of an engine and the end-effector tool, respectively. The arms are made out of aluminium ($E = 0.7 \cdot 10^{11}$ N/m^2, $\nu = 0.3$) and have length 1m. The initial dimensions are given in detail in the topology optimization section. Driving the manipulator the two arms show elastic deformations in the e_1e_2-plane and, as a result, the end-effector position $\boldsymbol{r}^{ef}(\boldsymbol{q}_r, \boldsymbol{q}_e)$ of the manipulator deviates from the desired semi-circular trajectory $\boldsymbol{r}^{ef}_d$, see Fig. 2(b).

4 Topology optimization

4.1 Optimization procedure

The simulation workflow used for the optimization resembles the procedure presented in Held and Seifried [2010] and is shown in Fig. 3. Regardless of the type of optimization, i.e. parameter, shape or topology optimization, as soon as the design parameters refer to the elastic bodies, the optimization procedures have to include the following steps.

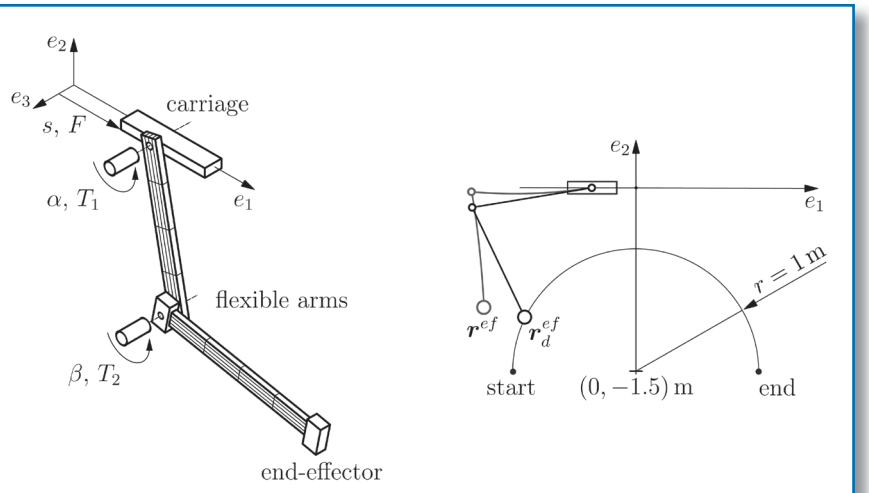

(a) Schematic representation of the investigated manipulator.

(b) Desired end-effector trajectory.

Figure 2:
Serial 2-arm testing manipulator and desired trajectory.

Starting from an initial design, at first a finite element model of the flexible body has to be created. Then a model reduction must be performed and the standard input data are calculated. Next the equations of motion of the flexible multibody systems have to be provided and the time simulation must be run. Finally, the objective function and existent constraints equations must be evaluated from the simulation results and passed to the optimizer. The latter suggests then an improved design and the simulation model is started over again until a stopping criterion is reached.

In this paper, the optimization procedure is mainly established using Matlab. That is, the simulation model as well as the optimizer are implemented in Matlab. However, within the simulation model, external programs such as ANSYS are called for the finite element analysis and the time simulation, respectively.

4.2 The SIMP approach

A common method for solving topology optimization problems is the SIMP approach. Thereby, the reference domain is discretized and continuous density-like parameters $\varkappa_i$ are introduced for each subdomain as design variables. Normally a subdomain is one finite element and the design variables are gathered in the vector $\boldsymbol{\varkappa} \in R^m$. Thus, the optimization problem can be formulated as a large scale sizing problem. The effective subdomain density and stiffness are computed as

$$\rho_i = \varkappa_i \rho_0 \quad \text{and} \quad E_i = \varkappa_i^p E_0, \qquad (6)$$

whereby ρ_0 and E_0 represent the density and the Young's modulus

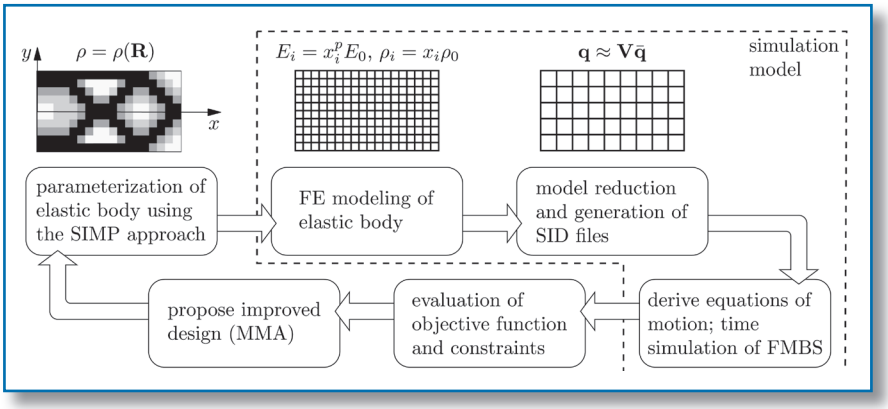

Figure 3:
Schematic representation of the optimization procedure.

of the solid material. In order to enforce a design which has only empty (0) and filled (1) subdomains, the stiffness is penalized by a power law with the exponent p.

As was mentioned in Section 2, one crucial step in the modeling of flexible multibody systems with the floating frame of reference formulation is the model reduction, which is performed to obtain the global shape functions. This is a major difference to classical topology optimization, where such a reduction step is not required. However, using the standard penalization law, localized modes may arise in low density areas, compare Pedersen [2000]. As a result, the modal reduction returns shape functions, which fail to approximate the elastic deformations. Thus, the penalization strategy for the stiffness is slightly adapted for very small values of x_i such that

$$E_i = \begin{cases} x_i^p E_0 & \text{for } 0.1 \le x_i \le 1 \\ x_i E_0/100 & \text{for } x_{min} \le x_i \le 0.1 \end{cases} \quad (7)$$

4.3 Optimization problem formulation

The tracking error $e(t)$ of the end-effector position at a specific time is measured by the Euclidean distance between the desired $\boldsymbol{r}_{\mathrm{d}}^{\mathrm{ef}}$ and the actual position $\boldsymbol{r}^{\mathrm{ef}}$. Since the application example is a planar manipulator, its error is given by

$$e(t) = \sqrt{\left(r_{x,d}^{ef}(t) - r_x^{ef}(t)\right)^2 + \left(r_{y,d}^{ef}(t) - r_y^{ef}(t)\right)^2}. \quad (8)$$

In order to lower tracking errors, a performance criterion has been defined, which relates the trakking behavior and the deformation energy c of the elastic body. Therefore, the tracking error is determined within the simulation time, see Fig. 4, and the first n maximal values of the tracking error are identified. After that, the according displacement fields $\boldsymbol{u}_j$, j =1, 2, ..., n can be recovered by multiplying the shape functions with the elastic coordinates

$$\boldsymbol{u}_j = \boldsymbol{\Phi}\,(\boldsymbol{R})\ \boldsymbol{q}\ (t_j). \quad (9)$$

With the displacement fields $\boldsymbol{u}_j$ and the stiffness matrix $\boldsymbol{K}$ of the unreduced finite element model, the compliance c can be computed and the overall optimization problem can be written as

$$\underset{\boldsymbol{x}\in\boldsymbol{R}^m}{\text{minimize}} \quad c(\boldsymbol{x}) \quad \text{with} \quad c = \sum_{j=1}^{n} \boldsymbol{u}_j^T \boldsymbol{K} \boldsymbol{u}_j = \sum_{j=1}^{n}\sum_{i=1}^{m} x_i^p \boldsymbol{u}_j^{i\,\mathrm{T}} \boldsymbol{K}_0^i \boldsymbol{u}_j^i$$

$$\text{subject to} \quad h(\boldsymbol{x}) = -V_0 + \sum_{i=1}^{m} x_i \le 0$$

$$\underline{\boldsymbol{x}} \le \boldsymbol{x} \le \overline{\boldsymbol{x}}, \quad (10)$$

whereby $\boldsymbol{K}_0^i$ is the local stiffness matrix of element i with Young's modulus E_0. Besides the minimization of the compliance c, a volume restriction h as well as the upper $\overline{\boldsymbol{x}}$ and lower $\underline{\boldsymbol{x}}$ bounds for the design variables are defined.
Since the compliance is computed from a set of selected displacement fields, the approach resembles the equivalent static load method by Kang and Park [2005]. A clear advantage of this procedure is that the highly expensive computation of the gradient can be avoided in contrast to functional objective functions. Instead, the sensitivity information is computed with respect to the equivalent static loads and can be found as

$$\frac{\partial c}{\partial x_i} = -p x_i^{p-1} \sum_{j=1}^{n}\sum_{i=1}^{m} \boldsymbol{u}_j^{i\,\mathrm{T}} \boldsymbol{K}_0^i \boldsymbol{u}_j^i. \quad (11)$$

using an adjoint variable approach, see Bendsøe and Sigmund [2003]. However, as a consequence the coupling between the design variables and the transient loads, which act on the elastic body, cannot be considered precisely.
Since topology optimization problems, and in particular the SIMP approach, lead inherently to large-scale optimization problems, they are commonly tackled by gradient-based optimizers. Here, the Method of Moving Asymptotes presented by Svanberg [1987] is employed.

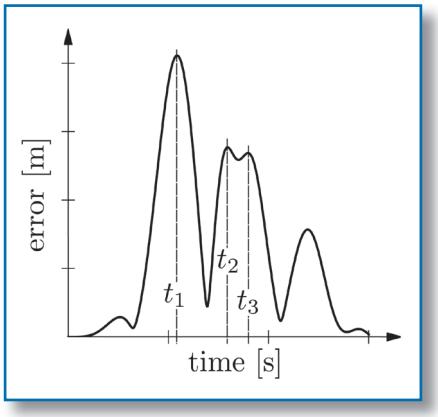

Figure 4:
Load case identification.

4.4 Optimization result

The topology optimization procedure is used to optimize the

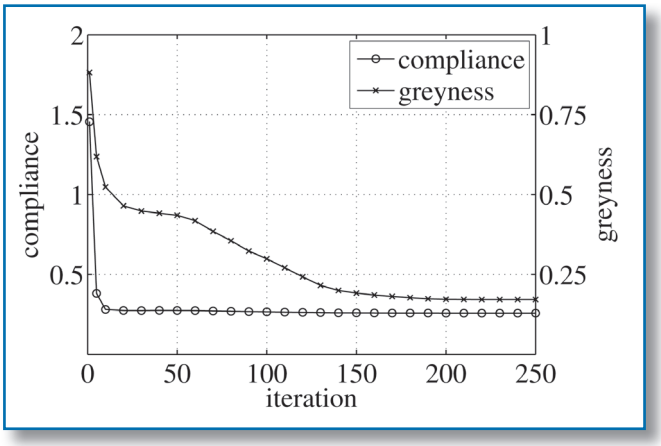

Figure 5:
Convergence of compliance and greyness.

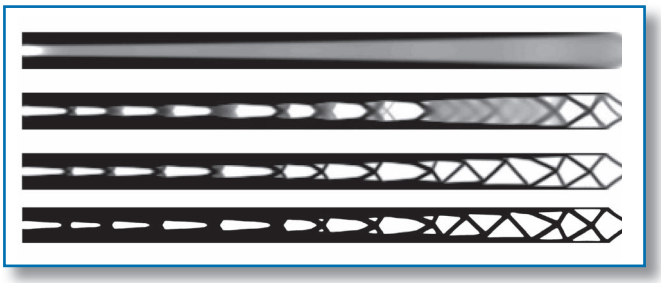

Figure 6:
Arm design after 10, 100, 200 iterations and final post-processed design.

design of the first flexible arm of the application example, see Fig. 2. A planar reference domain is defined to be 1 m and 0.06 m in the x-and the y-direction, respectively. It is discretized using 400x24 finite elements, which possess four nodes having two translational degrees of freedom each. The thickness z is constant and chosen as 10 mm.

Starting with a homogeneous material distribution of $x_i = 0.7$ the optimization loop has converged after roughly 200 iterations. To analyze the resulting designs, the compliance and the greyness are used. The latter is computed as

$$g(\boldsymbol{x}) = \frac{4}{m}\sum_{i=1}^{m}(1-x_i)x_i \qquad (12)$$

and quantifies the amount of intermediate densities, see Sigmund [2007]. These intermediate densities are physically not meaningful and have to be removed for a viable final design. Fig. 5 shows, that the compliance drops strongly within the first 10 iterations. In these first iterations, the basic layout of the arm emerges and the flexible arm is stiffened against bending, see Fig. 6. In the following iterations, the compliance decreases, but very slowly. In contrast, it takes significantly more iterations for the greyness to converge, because the cross struts are formed slowly. In a post-processing step, the remaining intermediate densities are eliminated to generate the final design, see Suresh [2010]. It can be shown that the optimization of the arm improves the tracking behavior of the system, see Fig. 7. The maximal end-effector tracking error is reduced from 11.6 mm to 7.1 mm and the averaged deviation from 3.79 mm to 1.56 mm.

5 Conclusions

In this work a topology optimization procedure for the optimal design of lightweight machine design is presented. The optimization is performed with regard to simulation models which employ the method of flexible multibody systems. In this way all significant structural dynamic effects during the working motion are included. For computational effciency the floating frame of reference formulation in conjunction with model reduction is used. The latter demands for a change in the penalization scheme of the SIMP approach, in order to avoid localized modes, which impair the results of the flexible multibody simulation.

Applying the procedure to optimize the flexible arms of a manipulator it can be shown that the system performance, here the tracking behavior, is improved significantly. For example, after topology optimization the maximal end-efector tracking error is reduced by almost 40% without increasing the system's mass. Thus, it is concluded that the topology optimization procedure is suited to adapt the mechanical design with regard to dynamic loads and improve the performance of the mechanical design.

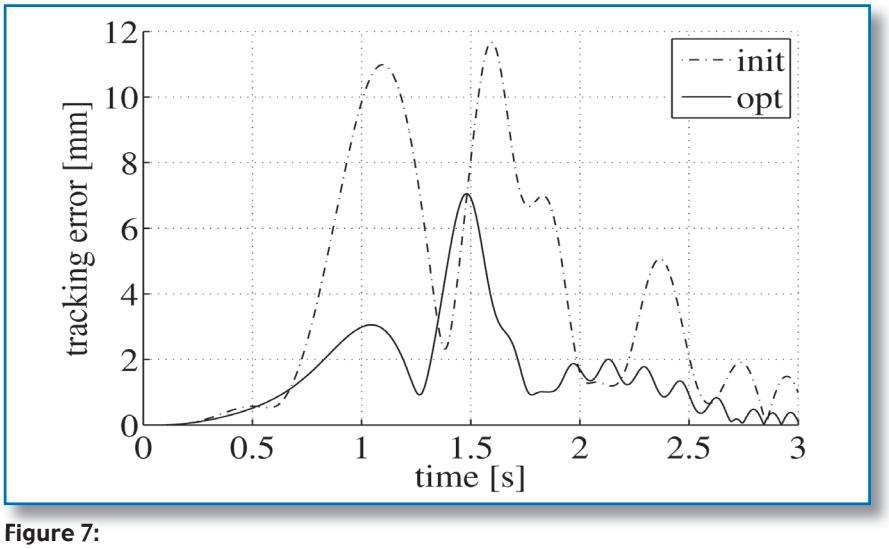

Figure 7:
End-effector error of topology optimized design.

References

Albers, A., Ottnad, J., Weiler, H., Haeussler, P., Methods for Lighweight Design of Mechanical Components in Humanoid Robots. IEEE-RAS International Conference on Humanoid Robots, Pittsburg, Pennsylvania, USA, 2007.

Kang, B.S.; Park, G.J.: Optimization of Flexible Multibody Dynamic Systems Using the Equivalent Static Load Method. AIAA Journal, Vol. 43, 2005.

Brüls, O., Lemaire, E., Duysinx, P., Eberhard, P., Optimization of Multibody Systems and Their Structural Components. Multibody Dynamics: Computational Methods and Applications, K. Arczewski, W. Blajer, J. Fraczek, M. Wojtyra (Eds.), Computational Methods in Applied Sciences, Vol. 23, Springer, 2011, pp. 49-68.

Lehner M., Modellreduktion in elastischen Mehrkörpersystemen (in German), Shaker Verlag, Aachen, 2007.

Bendsøe, M., Sigmund, O., Topology Optimization -Theory Methods and Applications. Berlin, Springer, 2003.

Shabana, A., Dynamics of Multibody Systems. Cambridge University Press, Cambridge, 2005.

Schwertassek, R., Wallrapp, O., Dynamik flexibler Mehrkörpersysteme (in German). Vieweg, Braunschweig, 1999.

Wallrapp, O., Standardization of Flexible Body Modeling in Multibody System Codes, Part 1: Definition of Standard Input Data. Mechanics of Structures & Machines, Vol. 22, No. 3, pp. 283–304, 1994.

Spong, M., Hutchinson, S., Vidyasagar, M., Robot Modeling and Control. John Wiley & Sons, Hoboken, 2006.

Seifried, R., Held, A., Dietmann, F.: Analysis of Feed-Forward Control Design Approaches for Flexible Multibody Systems. Journal of System Design and Dynamics, Vol. 5, No. 3, pp. 429-440, 2011.

Seifried, R., Held, A., Integrated Design Approaches for Controlled Flexible Multibody Systems. Proceedings of the ASME 2011 International Design Engineering Technical Conferences (IDETC/CIE 2011), August 29-31, 2011, Washington, DC, USA.

Held, A., Seifried, R., A Procedure for Shape Optimization of Controlled Elastic Multibody Systems. Proceedings of the Seventh International Conference on Engineering Computational Technology, B. Topping, J. Adam, F. Pallares, R. Bru, M Romero (Eds.), Civil-Comp Press, Stirlingshire, paper ID 100, 2010.

Pedersen, N.L., Maximization of Eigenvalues using Topology Optimization. Structural and Multidisciplinary Optimization, Vol. 20, pp. 2–11, 2000.

Svanberg, K., The Method of Moving Asymptotes -A New Method for Structural Optimization. International Journal for Numerical Methods in Engineering, 1987, 24, 359–373.

Sigmund, O., Morphology-based Black and White Filters for Topology Optimization. Structural and Multidisciplinary Optimization, Vol. 33, pp. 401–424, 2007.

Suresh, K., A 199-line Matlab Code for Pareto-optimal Tracing in Topology Optimization. Structural and Multidisciplinary Optimization, Vol. 42, pp. 665–679, 2010.

Soft structures with fluid interaction

M. Schörgenhumer[1], P.G. Gruber[2], K. Nachbagauer[3] and J. Gerstmayr[2]
[1] Austrian Center of Competence in Mechatronics GmbH
[2] Linz Center of Mechatronics GmbH
[3] University of Applied Sciences Upper Austria

Abstract

The interaction of fluids with solids – *fluid-structure interaction* (FSI) – can be observed in a large variety of natural phenomena and technical applications, ranging from the macroscale down to the microscale. Hence, the development of numerical methods to model and simulate FSI problems is both an important as well as a challenging task. In the present work, we discuss an approach to FSI based on the coupling of fexible multibody systems with fluids represented by a meshfree particle-based method, with the focus on fluid interaction with highly fexible fibers.

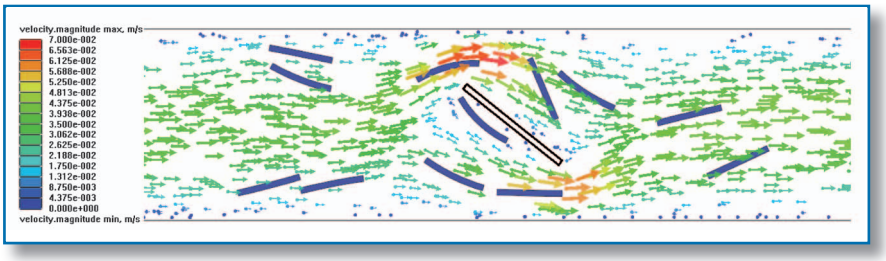

Figure 1:
Flexible fibers (blue) in a channel fow from left to right around a rigid obstacle (white bar), including mechanical contact. The vector plot represents the flow velocity field.

1 Introduction

Fluid-structure interaction plays an important role in a wide range of scientific fields and industrial applications, such as wind-induced vibrations of buildings or bridges, fexible valves or other fexible structures in machines, the motion of particles or fibers in a flow, problems in biomechanics (e.g. blood fow in fexible vessels), or applications in naval and offshore engineering involving wave motion and free-surface flows.

Up to now, numerous computational approaches to FSI have been developed (see, e.g., Galdi and Rannacher [2010]; Bungartz, Mehl, and Schäfer [2010]; Hou, Wang, and Layton [2012]). However, complex systems involving large structural displacements or several, possibly mutually interacting mechanical components still pose a formidable challenge regarding numerical modeling and simulation. In the approach presented in this work, fexible multibody systems are coupled with fluids simulated by the meshfree particle-based method smoothed particle hydrodynamics (SPH), with an implementation based on simulator coupling. The components of the multibody system interact with the fluid, i.e., the SPH particles, via surface potentials which generate appropriate mutual repulsive and viscous forces. While advanced methods from multibody dynamics provide an efficient and stable simulation of very general mechanical systems, the particle-based representation of the fluid can basically handle arbitrary changes in geometry or topology of the domain, as well as free fluid surfaces. Hence, the scope of our approach is of a very general kind. On the one hand, conventional problems of both computational solid as well as fluid mechanics are covered, either independently or coupled in the context of fluid-structure interaction. On the other hand, with the framework of multibody system dynamics as background, we are also aiming at complex *mechatronical* systems which involve FSI, but additionally may include actuators, drives, control, and other embedded systems. Note that many of these cases are highly nonlinear and exhibit complex interactions and dynamical behavior. Therefore, it is often not admissible to employ simplifed or reduced modeling, but rather neccessary to account for the full system by means of a fully coupled approach. Regarding numerical examples and applications, in the present work we investigate fluid interaction with highly flexible fibers, including mutual mechanical contact. The fibers are modeled using beam finite elements, which is not only efficient, but also brings along particular benefits with respect to stability and the smoothness of the fiber surface even in case of large deformation. Section 3 covers an overview of those beam formulations, Section 4 some information on the method SPH as well as an outline of our coupling concept, respectively; the numerical examples are presented in Section 5.

2 Soft structures

The particular choice of FE discretization of the soft structures has a crucial efect on efficiency and accuracy of the final FSI simulation, since soft structures imply particular geometrical and consti-

tutional nonlinearities. In many biomechanics applications soft, structures (such as membranes, tissues, fibers, arteries, ligaments, tendons) undergo large deformations and obey nonlinear material laws (e.g., viscoelasticity, elastoplasticity, viscoplasticity). Whenever we are interested in the simulation of very thin structures, a class of elements based on the so called *absolute nodal coordinate formulation* (ANCF) offers great advantages. The basic idea of finite elements based on the ANCF is the usage of nodal displacements and slopes as degrees of freedom instead of rotational parameters. Moreover, the use of absolute nodal coordinates leads in general to a constant mass matrix and is therefore preferable in dynamic analysis.

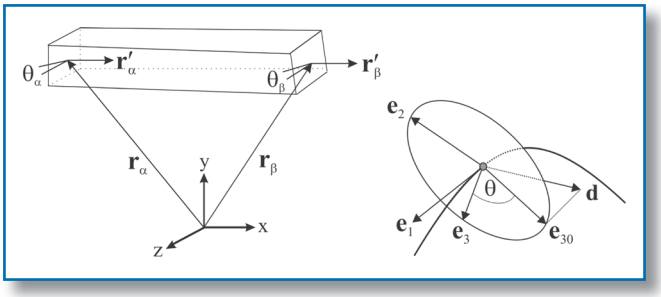

Figure 2:
Nodal degrees of freedom (left) and defnition of the local frame at an arbitrary point on the beam axis (right).

Note, that a further beneft of ANCF elements particularly in fluid structure interaction problems is due to the typically high continuity of the approximate solution. Hence a smooth surface geometry along element boundaries is provided even for very coarse discretizations.

2.1 An ANCF beam element for the modeling of soft structures

In the ANCF, there have been only few achievements for the modeling of 3D and large deformation Bernoulli-Euler beams with torsional deformation up to now. A signifcant approach has been presented by Gruber et al. [2013], which is used here in the fluid-structure interaction examples. The deformation of the element is described by means of displacement vector, axial slope and axial rotation parameter per node. The element is based on the Bernoulli-Euler theory and can undergo coupled large deformation axial extension, bending and torsion.

Singularities – which are typically caused by such parameterizations – are overcome by a director per element node. In order to keep the number of unknowns low, the director is updated after each computed step, but it is known during the computation of the step. Thin and very fexible structures can be modeled easily due to the continuity at the nodes. A detailed convergence analysis by means of various numerical static and dynamic examples and comparison to analytical solutions has shown the performance and accuracy of the element, see Gerstmayr and Irschik [2008] or Gruber et al. [2013]. The orientation of the cross section is parameterized in terms of a slope vector and a rotation parameter. The advantage of such a formulation is a simple expression for the inertia terms, which leads to a constant mass matrix and avoids nonlinear coupling in the inertia terms. Nevertheless, the element includes all geometrically nonlinear terms.

2.1.1 Geometry

The geometry of the beam is described by a curve, representing the beam's axis, and a cross section at each point of this axis, see Fig. 2. The axial position **r** and the torsional angle θ are interpolated

$$\begin{bmatrix} r_x & r_y & r_z & \theta \end{bmatrix}^T = \begin{bmatrix} \mathbf{S}_r & 0 \\ 0 & \mathbf{S}_\theta \end{bmatrix} \mathbf{q}, \qquad (1)$$

by means of cubic shape functions $\mathbf{S}_r$ and linear shape functions $\mathbf{S}_\theta$ between their nodal values

$$\mathbf{q} = \begin{bmatrix} \mathbf{r}_\alpha^T & \mathbf{r}'^T_\alpha & \mathbf{r}_\beta^T & \mathbf{r}'^T_\beta & \theta_\alpha & \theta_\beta \end{bmatrix}^T,$$

with α denoting the first, and β the second node index, see the left drawing in Fig. 2 or for more details Gruber et al. [2013]. In order to have a uniquely defined orientation of the cross section about the beam axis direction $\mathbf{e}_1 = \frac{\mathbf{r}'}{|\mathbf{r}'|}$ at an arbitrary point on the elastic line, a director **d** is utilized. With help of this vector, the local frame $\mathbf{A} = [\mathbf{e}_1\ \mathbf{e}_2\ \mathbf{e}_3]$ is defined by the projection of **d** into the normal plane of $\mathbf{e}_1$, and a subsequent rotation around a torsional angle θ, see the right drawing in Fig. 2. Due to the director approach, geometric singularities in the calculation of the local frame may be avoided, as long as the director is not collinear with the beam axis. A safe strategy to avoid this situation is to successively update the director at the FE-nodes at every load/time step. As experienced throughout many simulation examples, a simple projection of the directors at the FE-nodes into the cross section of the beam is sufficient. Summarizing, the geometry of a Bernoulli-Euler beam can be fully described by the axial position **r**, slope **r'**, and cross section orientation angle θ relative to the projected director **d**. However, geometric singularities might occur, if the slope **r'** becomes collinear with the director **d**. A safe strategy for preventing singularities throughout the deformation process using an updating procedure is addressed in the work by Gruber et al. [2013]. Due to the continuity of the axial slope and rotational angle, these elements lead to smooth structures.

2.1.2 Equations of motion

The full equations of motion are given by the well known Lagrange equations of the second kind. With the principle of virtual work applied to the one-dimensional Cosserat continuum the strain energy can be shown to be an additive function of two strain measures, one responsible for shear and axial extension, and the second one responsible for bending and torsion. When neglecting shear deformation, the resulting energy function reads

$$\Pi = \frac{1}{2}\int_{-L/2}^{L/2} \left(EA\varepsilon^2 + GJ\kappa_1^2 + EI_y\kappa_2^2 + EI_z\kappa_3^2 , \right) d\xi \,. \tag{2}$$

Here, conforming to Simo and Vu-Quoc [1986], the axial extension is described by the axial strain

$$\varepsilon = \frac{|\mathbf{r}'| - |\mathbf{r}_0'|}{|\mathbf{r}_0'|} \tag{3}$$

with $\mathbf{r}'$ and $\mathbf{r}_0'$ denoting the axial slope vector in the deformed and undeformed state, respectively, and the torsional strain

$$(\kappa_i)_{i=1}^3 = \frac{1}{2}\mathbf{A}^T \sum_{j=1}^{3} \mathbf{e}_j \times \mathbf{e}_j' \,, \tag{4}$$

for a straight beam in reference confguration. The kinematic terms, i.e., the mass matrix and the quadratic velocity vector, are derived from the kinetic energy as functions of $\mathbf{q}$ and $\dot{\mathbf{q}}$. Due to the consideration of the torsional parameters in the geometrical description, the mass matrix of the element finally depends on $\mathbf{q}$, which is exceptional in the class of ANCF elements. A constant approximation of the mass matrix and a reduced integration for the assembling of the quadratic velocity vector are discussed also in Gruber et al. [2013]. Let us finally conclude that the elastic forces and kinetic terms contain all geometrically nonlinearities according to the Bernoulli-Euler beam theory and allow the modeling of large deformations including torsion of highly fexible bodies as in the present investigations. In the following examples of Sec. 5 also *2D* elements are used. Let be mentioned, that starting from the geometrical and constitutional description of the beam as outlined in this section, the *2D* case may be recovered straight forward.

3 Modeling of fluids and fluid–structure interaction

3.1 Smoothed particle hydrodynamics

SPH is a Lagrangian meshfree particle-based method with origins in the context of astro-physical problems involving gas dynamics and high-speed collisions in the 1970s. Later, it was established as a field of interest in computational fluid dynamics by Monaghan [1994], and has become increasingly popular with a wide range of applications, such as free-surface or multiphase fows, coastal hydrodynamics and off-shore engineering, microfluidics, biomechanics, and, moreover, fluid-structure interaction (cf. Liu and Liu [2010]). In the framework of SPH, the fluid domain is divided into small volume fractions each of which is represented by one discrete fluid particle associated with a mass, density, and a corresponding volume. Of course, each particle has a specifc position and velocity, and furthermore may carry the value of field quantities such as the pressure, energy, or temperature. At any given point in the domain, the value of a continuous field variable, or, more generally, any continuous function defned on the fluid domain, is approximated by means of an unstructured interpolation – simplifying, a weighted sum – over the discrete values associated with the particles in the vicinity of that point. In this sense, the particles play the role of the nodes of any mesh-based method, such as classical continuum finite elements, and the weighting function, also called *smoothing kernel* of the interpolation is more or less analogous to the corresponding shape functions (for a sketch cf. Fig. 3). Based on that, the governing equations of fluid dynamics, the Navier-Stokes equations, can be discretized in Lagrangian form, which essentially reduces the continuous problem to the explicit computation of the dynamics of a set of discrete, mutually interacting particles – much like particle simulations in classical molecular dynamics – along with the time evolution of the particle density and energy. Due to its purely Lagrangian particle nature, the main benefts of SPH lie with the simplicity and flexibility with respect to complex, time-dependent fluid domains, as in the context of free-surface problems, waves, sloshing, and particularly, fluid-structure interaction involving large structural displacements, rotation, and/or deformation. Here, conventional mesh-based approaches would necessitate some kind of interface tracking, along with immersed boundary or immersed domain techniques on non-con-

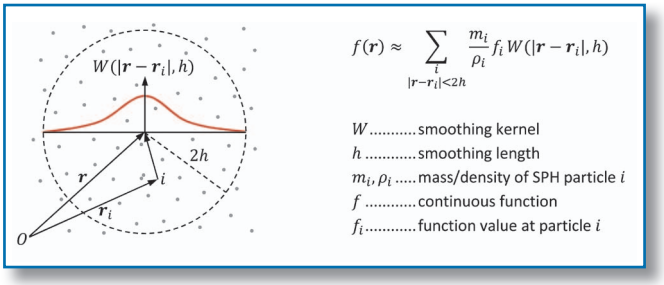

Figure 3:
SPH particle approximation of a continuous function $f(\mathbf{r})$.

forming grids, or conforming-mesh methods such as arbitrary Lagrangian-Eulerian formulations with appropriate mesh movement and remeshing (cf., for instance, Hou, Wang, and Layton [2012]). In contrast to that, the particle distribution in SPH automatically represents both the geometry as well as the "mesh" of the fluid domain at any time, hence providing simplicity as well as efciency.

On the other hand, the accuracy of the SPH approximation depends on the particle distribution and, in the usual formulations, is of low order, especially in the vicinity of boundaries or interfaces (see also Liu and Liu [2010]). Therefore, in order to obtain a certain degree of accuracy, relatively high spatial resolutions, i.e. large numbers of particles (particularly in three spatial dimensions) are required compared to conventional mesh-based methods. However, this is remedied by the fact that the discretized equations are typically integrated explicitly, and, moreover, the system is very well suited for parallelization, which allows for the implementation of fast and highly efficient solvers. Other (problematic) issues in SPH, which are still under investigation, regard the treatment of walls, or in general, impervious boundaries, as well as any Eulerian boundary condition on a spatially fixed domain.

For further details concerning the theory and applications of SPH see, for instance, Liu and Liu [2003], or review papers such as Monaghan [2005]; Liu and Liu [2010].

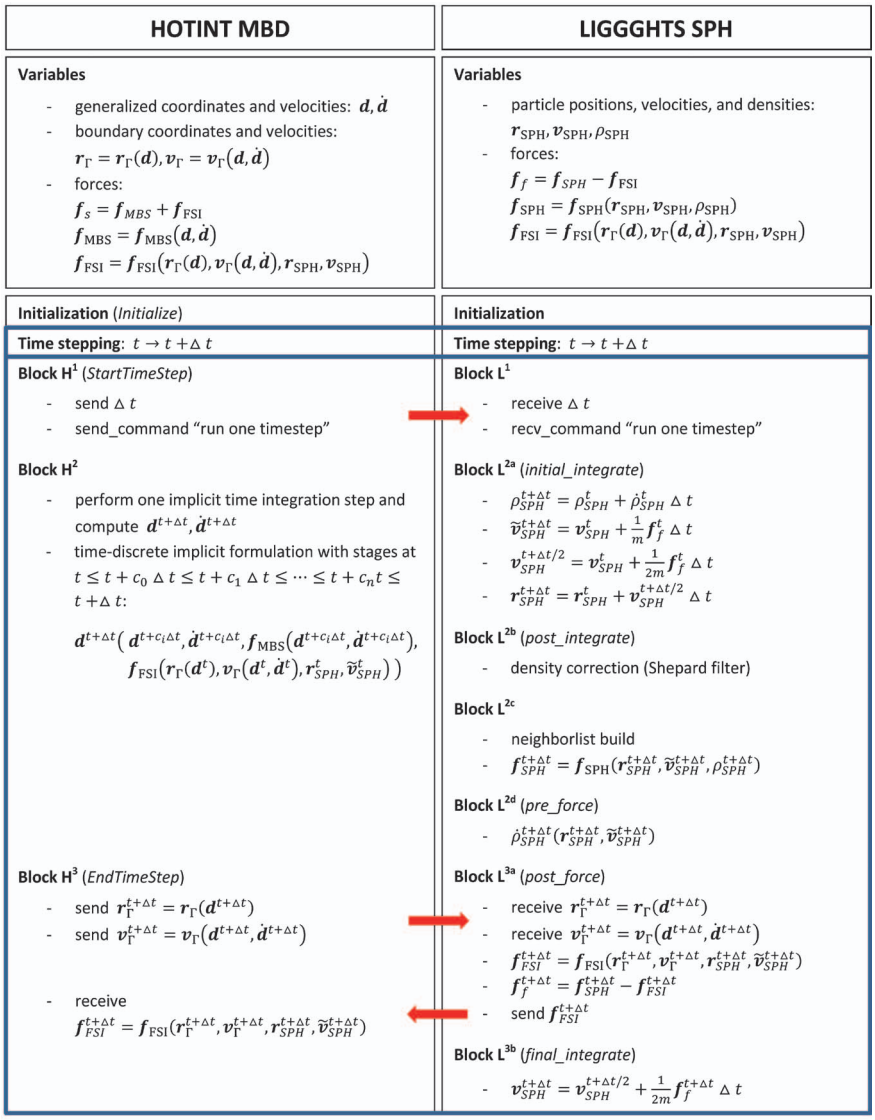

Figure 4:
HOTINT (left-hand side, multibody dynamics) is coupled with LIGGGHTS (right-hand side, SPH) via TCP/IP for both data transfer and synchronization (red arrows).

3.2 Multibody systems with fluid-structure interaction

As a versatile approach to FSI flexible multibody systems are coupled with viscous fluids modeled by SPH, accounting for the two basic requirements on any fluid-structure interface – the kinematic boundary conditions, and the equilibrium of forces. The former requires the relative normal and tangential fluid velocity to vanish on any solid impervious boundary – a rigid, stationary wall or the surface of a moving, deforming body, for instance – and is also known as the *no-penetration* and *no-slip* condition. The latter states that the mechanical stress distribution on each boundary is equal to the local pressure and shear forces in the fluid.

In this work we have adapted an approach based on Müller et al. [2004], where appropriate fluid-structure interaction forces are generated between the fluid, i.e., the SPH particles, and any fluid-structure interface by two short-ranged potentials defned over all boundaries – one to prevent the particles from penetrating the wall, and the other one to account for the no-slip condition. The forces are computed numerically from integrals over the surface of each body in contact with the fluid, via Gauss-Legendre quadrature on surface meshes with adaptive refinement. Note that this approach is applicable in two as well as three spatial dimensions, and can be – as the SPH simulation itself – parallelized effectively. See Schörgenhumer, Gruber, and Gerstmayr [2013] for further details.

Numerically, we are confronted with two very diferent challenges: On the one hand, the multibody dynamics are described by a comparatively small, but coupled nonlinear system of differential-algebraic equations, while on the other hand, the fluid dynamics in terms of SPH (as well as the FSI formalism) basically are reduced to the computation of the motion of a great many, yet "simple" particles. Regarding the implementation, we are using two simulation tools, "HOTINT" (cf. Gerstmayr et al. [2013], see also www.hotint.org) for the multibody system dynamics and "LIGGGHTS" (cf. www.liggghts.com) for SPH, which run on two different machines and communicate via TCP/IP. In the sense of a weakly-coupled scheme, in each time step geometrical data (i.e., positions and velocities of the nodes of the surface meshes) is passed from HOTINT to LIGGGHTS, which then computes the FSI forces and finally sends back the corresponding counterforces to HOTINT. Here, HOTINT is used as the server application, while the client actually is a wrapper code which calls LIGGGHTS as external library and communicates with the server. Hence, the control of the coupled simulation and communication, the evaluation, visualization, and post-processing of the simulation data, as well as the whole problem set-up is done in HOTINT.

A detailed sketch of the coupling scheme is shown in Fig. 4, with the right-hand side of the picture corresponding to HOTINT, and the left-hand side to LIGGGHTS, respectively. The variables, i.e., the generalized coordinates describing the multibody system, and the positions, velocities and densities of the SPH particles discretizing the fluid, are listed in the upper box along with the forces. The latter comprise f_s as the sum of the internal forces of the multibody system f_{MBS} and the forces due to the fluid-structure interaction f_{FSI} on the one hand, and f_f consisting of the internal forces f_{SPH} in the SPH particle system and, correspondingly, the FSI contribution f_{FSI} on the other hand.

For more information concerning the coupling on the level of the mathematical model or the implementation, the kinematic boundary conditions and the dynamic equilibrium, as well as the surface discretization and the numerical computation of the fluid-structure contact, again refer to Schörgenhumer, Gruber, and Gerstmayr [2013].

4 Numerical simulations

Rigid or fexible cells or fibers immersed in fluid flow play an important role in various scientifc and industrial fields, ranging from biomechanics (e.g. red blood cells in microcappilares) and microfluidics (e.g. cell identification, cytometry) to industrial applications (e.g. production of fiber-reinforced or composite materials). Therefore, concludingly we present several examples involving highly flexible fibers, modeled with beam finite elements within the multibody formalism (see also Subsection 3.1). Those elements combine computational efficiency, stability, as well as a smooth surface even in highly non-linear cases of large deformation, and hence are superior to conventional approaches such as classical continuum finite elements.

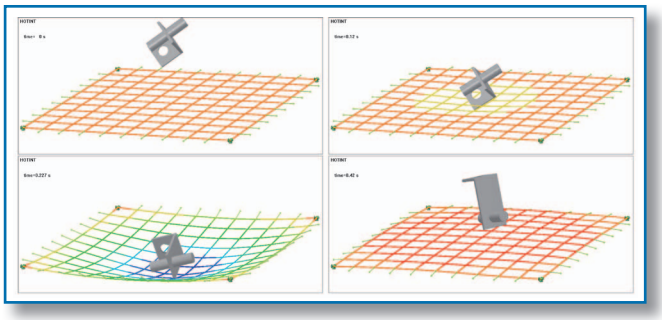

Figure 5:
The figure shows four plots demonstrating the impact of an obstacle in a soft web, see Example 5.1.

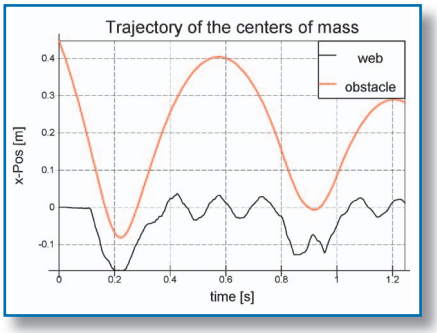

Figure 6:
Trajectory of the obstacle and web in Example 5.1. The curve of the obstacle reflects clearly the effect of the dampers applied to the web.

4.1 Contact between rigid body and soft structure

Before turning to fully coupled fluid-structure interaction examples, a first purely solid mechanics test is presented. Here we study the collision of a rigid obstacle with a soft web constructed of ANCF beam elements as outlined in Section 3.1. The material parameters of the web have been chosen particularly soft in order to obtain high deformations in the dynamic simulation. The web is spatially fixed at the corners, and damped at each of its boundary nodes. The elements performed fast and stable (see Fig. 5 and 6) in this solid contact example, and approve their applicability also in the following FSI problems.

4.2 Injection process

In this example, a simple injection process in *2D* with a highly viscous fiber-filled fluid is simulated. A rigid piston is used to pump the fluid through a channel into the

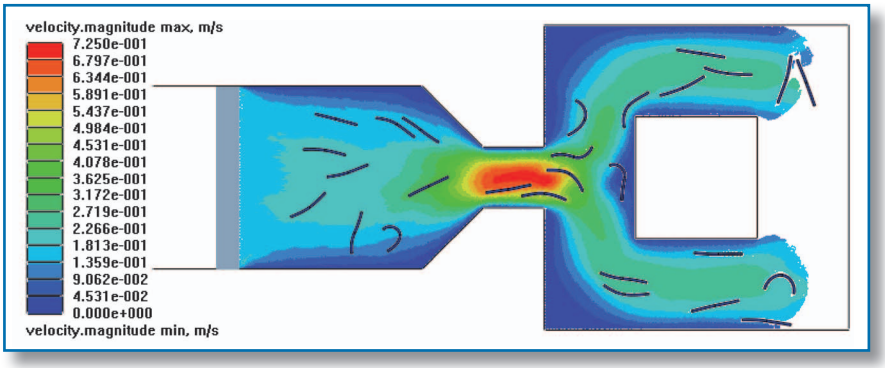

Figure 7:
Snapshot of an injection process of a highly viscous fluid with immersed fexible fibers into a mold; the piston (grey) is moving from left to right. The color map corresponds to the fow speed.

mold. The fibers are modeled by ANCF beam elements (see also Subsection 3.1), and mutual mechanical contact between the fibers, as well as fiber-wall contact is included in the multibody formulation. See Fig. 7 for illustration. With such simulations the spatial distribution, placement and orientation of fibers can be investigated, which particularly is of interest in industrial production processes of fiber-reinforced materials.

4.3 Flow through a fiber array

Here, we present one test case in *3D*, with a fluid moving through an array of fibers as sketched in the left-hand side of Fig. 8. The fluid is driven by gravity, and the fibers are modeled with *3D* ANCF beam elements as discussed in Subsection 3.1, with clamped-end boundary conditions. Linear triangular surface meshes were generated and imported as STL files for the outer geometry as well as the cylindrical surface of the fibers in the undeformed reference confguration. Furthermore, note that this example is also a free-surface flow problem; snapshots of a simulation are shown in the right-hand side of Fig. 8, as well as in Fig. 9.

5 Conclusions

The presented approach to fluid-structure interaction is aimed at both effciency as well as the applicability to a wide range of FSI problems. Based on the framework of fexible multibody system dynamics and particle-based fluid mechanics it is particularly suitable for the numerical modeling and simulation of complex mechanical or mechatronical systems with fluid interaction. As test cases in this work, using advanced beam fnite element formulations, interactions of fluids with highly flexible fibers were investigated.

Acknowledgements

The authors M. Schörgenhumer, P.G. Gruber, and J. Gerstmayr gratefully acknowledge the support of this work by the K2-Comet Austrian Center of Competence in Mechatronics GmbH (ACCM).

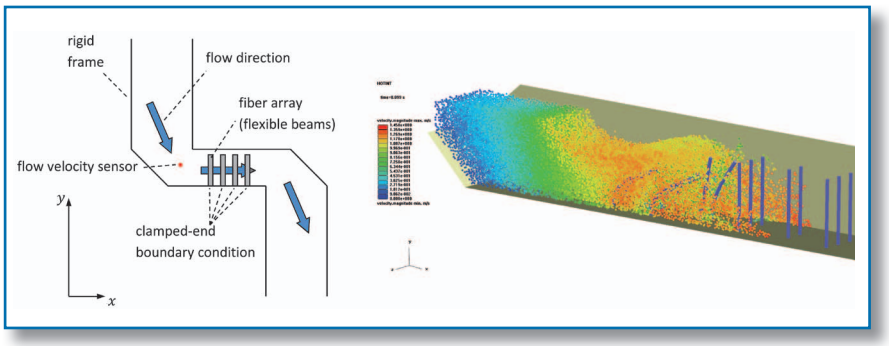

Figure 8:
Left: Sketch of the system: Fluid is moving through an array of flexible fibers inside a rigid-wall geometry, driven by gravity in negative y-direction. A sensor is placed centrally in front of the fibers to measure the flow velocity. Right: Snapshot during a simulation: The fibers (light blue) exhibit large deformation in the flow. For better visibility, only a fraction of the SPH particles is plotted; the colors correspond to their speed.

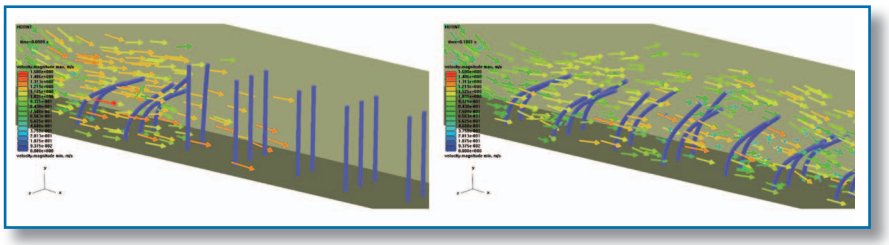

Figure 9:
Snaphshots during a simulation at two different times. The vector plot corresponds to the flow velocity field.

References

Galdi P.G. and Rannacher R. (eds.), Fundamental Trends in Fluid-Structure Interaction. Contemporary Challenges in Mathematical Fluid Dynamics and its Applications. World Scientifc Publishing 2010.

Bungartz H.J., Mehl M., and Schäfer M. (eds.), Fluid-Structure Interaction II: Modelling, Simulation, Optimisation. Springer 2010.

Hou G., Wang J., and Layton, A., Numerical Methods for Fluid-Structure interaction – A Review. Commun. Comp. Phys., 12, 337-377, 2012.

Simo J.C. and Vu-Quoc L., A Three-Dimensional Finite-Strain Rod Model. Part II: Computational Aspects. Comp. Meth. Appl. Mech. Eng., 58, 79-116, 1986.

Gruber P.G., Nachbagauer K., Vetyukov Y., and J. Gerstmayr, A novel director-based Bernoulli-Euler beam fnite element in absolute nodal coordinate formulation free of geometric singularities, submitted to Journal of Mechanical Sciences – An Open Access Journal for Theoretical and Applied Mechanics.

Gerstmayr J. and Irschik H., On the correct representation of bending and axial deformation in the absolute nodal coordinate formulation with an elastic line approach. J. Sound Vib., 318, 461-487, 2008.

Monaghan J.J., Simulating Free Surface Flows with SPH, J. Comp. Phys., 110, 399-406, 1994.

Liu M.B. and Liu G.R, Smoothed Particle Hydrodynamics (SPH): an Overview and Recent Developments, Arch. Comp. Meth. Eng., 17, 25-76, 2010.

Liu G.R. and Liu M.B., Smoothed Particle Hydrodynamics. World Scientifc Publishing 2003.

Monaghan J.J., Smoothed particle hydrodynamics. Rep. Prog. Phys., 68, 1703-1759, 2005.

Müller M. et al., Interaction of fluids with deformable solids. Comp. Anim. Virtual Worlds, 15, 159-171, 2004.

Schörgenhumer M., Gruber P.G., and Gerstmayr J., Interaction of fexible multibody systems with fluids analyzed by means of smoothed particle hydrodynamics, Multibody Syst. Dyn., 30, 53-76, 2013.

Gerstmayr J. et al., HOTINT – A Script Language Based Framework for the Simulation of Multibody Dynamics Systems. In: Proceedings of the ASME 2013 IDETC/CIE, Portland, OR, USA, 2013.

MARINE 2013

V. International Conference on Computational Methods in Marine Engineering

The 5th International Conference on Computational Methods in Marine Engineering took place at premises of the "Patriotische Gesellschaft" in Hamburg in May 2013 with more than 175 participants coming from 29 countries.

The conference was organized by Birgitt Brinkmann from the Institute of Hydraulic and Port Engineering of Leuphana University, Lüneburg together with Peter Wriggers from the Institute of Contiuum Mechanics of Leibniz Universität Hannover.

The objective of MARINE 2013 was to be a meeting place for scientists and engineers developing computational methods related to complex problems in marine engineering. The objectives included applications within the maritime and offshore industry as well as scientific and engineering challenges related to the marine environment and its logistics. The conference goal was to make a step forward in the formulation and computational solution of marine engineering problems accounting for all the complex couplings involved in the physical and practical aspects of the problems.

Seven plenary lectures and 134 contributed presentations presented the state-of-the-art of marine engineering. The topics of the plenary lectures ranged from ship hull design and optimization, the magnitude of loads acting on offshore structures, wave analysis in deterministic and stochastic sense, computational models for offshore wind turbines up to optimal asset integrity management of marine structures. This range of subjects was completed by associated minisymposia and contributed lectures.

As for the social program the participants enjoyed a sunny boat trip through the canals and harbor of Hamburg, upstream river Elbe to a charming thatched farmhouse restaurant. Here scientific discussions between all participants found a delicious culinary forum.

The VI. Conference of MARINE will take place June 15–17, 2015 in Rome.

EURO:TUN 2013

3rd International Conference on Computational Methods in Tunneling and Subsurface Engineering

The EURO:TUN conferences are organized as Thematic Conferences of the ECCOMAS. The Ruhr-University in Bochum, Germany hosted the 3rd International Conference on Computational Methods in Tunneling and Subsurface Engineering during April 17–19, 2013. It attracted more than 130 participants from 25 countries both from academia and practice. Presentations and discussions at the three conference days provided a forum for the discussion, assessment and review of latest advances in research, new developments and applications of numerical models and computational methods in tunneling and subsurface engineering. Besides contributed presentations in regular sessions, presentations have been given in 14 invited minisymposia addressing specific topics of particularly high relevance.

This year's EURO:TUN conference was closely connected to the Collaborative Research Center SFB-837 „Interaction Modeling in Mechanized Tunneling" installed at Ruhr-University Bochum. A special Joint Workshop of the RUB-SFB837 group with scientists from Tongji University and the Innovation and Knowledge Center (IKC) at Cambridge University was co-organized by Profs. H.W. Huang (Tongji University, China), K. Soga (Cambridge University, UK) and G. Meschke

(Ruhr-University Bochum, Germany) at April, 15th, 2013.

At this workshop, the latest results from research performed at the three institutions in the area of numerical modeling, new sensors and monitoring methods and experimental investigations in tunneling engineering have been exchanged.

The next joint RUB–SFB837–Tongji–IKC–Cambridge workshop will be organized in May 25th 2014 at Tongji University, Shanghai.

ECCOMAS Multibody Dynamics 2013

Continuing the very successful series of past ECCOMAS multibody conferences, the 2013 edition of the ECCOMAS Thematic Conference on Multibody Dynamics was held in Zagreb, Croatia, and organized by the University of Zagreb, Faculty of Mechanical Engineering and Naval Architectute, from July 1 – 4, 2013. 252 participants from 38 countries presented and discussed various topics concerning multibody dynamics in 13 sessions. The conference did provide a forum for discussions on the relevant research issues and served as a meeting point for the international researchers, scientists and experts from academia, research laboratories and industry. The hospitality of the city of Zagreb contributed to the conference success by providing culturally interesting and relaxing urban environment of the city that serves as an academical centre of the region for more than last 340 years.

IMSD 2012

Second Joint International Conference on Multibody System Dynamics

The Joint International Conference on Multibody System Dynamics (IMSD) took place at the Institute of Engineering and Computational Mechanics at the University of Stuttgart, Germany in May 29 – June 1, 2012.

Besides seven distinguished keynote lectures, 56 technical sessions were held, offering 192 technical presentations authored by more than 450 authors and 140 full papers were included to the Conference Proceedings. In total, 299 participants from 29 different countries participated in the IMSD 2012. In addition to providing the opportunity for a free exchange of high-level current information on the theory and applications of multibody systems, the spirit of cooperation was also encouraged by an interesting social program with a charming Conference Dinner in the Aquarium of the Stuttgart Zoo Wilhelma.

The 2nd Joint International Conference on IMSD Multibody System Dynamics

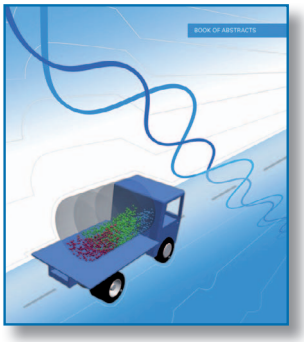

	GACM	ECCOMAS	IACM	USACM
2013	GACM 5 Hamburg 30 Sept - 2 Oct	TC - YIC 2 * Bordeaux 2 - 6 Sept	–	USNCCM 12 Raleigh 22 - 25 July
2014	–	ECCM V - ECFD VI - WCCM XI * Barcelona 20-25 July		–
2015	GACM 6	TC - YIC 3 *	–	USNCCM 13 San Diego 27 - 30 July
2016	–	ECCOMAS Congress VII * Crete June 2016	WCCM XII - APCOM Seoul 24 - 29 July 2016	–
2017	GACM 7	TC - YIC 4 *	–	USNCCM 14
2018	–	ECCM VI - ECFD VII *	WCCM XII Americas	–
2019	GACM 8	TC - YIC 5 *	–	USNCCM 15
2020	–	ECCOMAS Congress VIII *	WCCM XIV Europe	–

TC = Thematic Conferences, YIC = Young Investigator Conference, * = PhD Olympiad

WCCM XI – ECCM V – ECFD VI

The International Association for Computational Mechanics (IACM) and the European Community on Computational Methods in Applied Sciences (ECCOMAS) jointly organize the 11th World Congress on Computational Mechanics (WCCM XI), the 5th European Conference on Computational Mechanics (ECCM V) and the 6th European Conference on Computational Fluid Dynamics (ECFD VI). The congress will take place in the premises of the complex made up of the Palace of Congresses of Catalonia during July 20 – 25, 2014 and is locally organized by the Sociedad Española de Métodos Numéricos en Ingeniería – SEMNI (Spanish Association for Numerical Methods in Engineering). A very broad range of topics in computational solid and fluid mechanics is covered in 260 different minisymposia and one page abstracts can be submitted until November 29, 2013.

WCCM XI - ECCM V - ECFD VI
BARCELONA 2014

Further information is available at
http://www.wccm-eccm-ecfd2014.org.

Organizing Committee

Antonio Huerta (Co-chairman), Barcelona, Spain
Javier Oliver (Co-chairman), Barcelona, Spain
Eugenio Oñate (Co-chairman), Barcelona, Spain
Pedro Diez, Barcelona, Spain
Sergio Idelsohn, Santa Fe, Argentina
Carlos Mota Soares, Lisbon, Portugal
Manolis Papadrakakis, Athens, Greece
Jacques Periaux, Paris, France
Genki Yagawa, Tokyo, Japan
Tarek Zohdi, Berkeley, USA

IMPORTANT DATES

Deadline for presenting a one page abstract
November 29, 2013

Acceptance of the contributions
January 31, 2014

Deadline for submitting the full paper (not mandatory), **final acceptance and early payment**
February 28, 2014

iacm

IACM and ECCOMAS are pleased to announce the joint organization of

ECCOMAS

11th. World Congress on Computational Mechanics (WCCM XI)

and

5th. European Conference on Computational Mechanics (ECCM V)

6th. European Conference on Computational Fluid Dynamics (ECFD VI)

20 - 25 July 2014 - Barcelona, Spain

GAMM 2014

The 85th annual meeting of the International Association of Applied Mathematics and Mechanics (GAMM)

The 85th annual meeting of the International Association of Applied Mathematics and Mechanics (GAMM) is hosted by the Friedrich-Alexander University Erlangen-Nuremberg during March 10 – 14, 2014.

On the first day, the Prandtl lecture as well as three plenary lectures and the opening reception take place in the townhall in Fürth, while the rest of the conference happens at the South Campus of the University of Erlangen.

Five minisymposia, five young researchers minisymposia and 24 regular sessions cover the scientific development in all areas of applied mathematics and mechanics, see ***http://jahrestagung.gamm-ev.de*** for details.

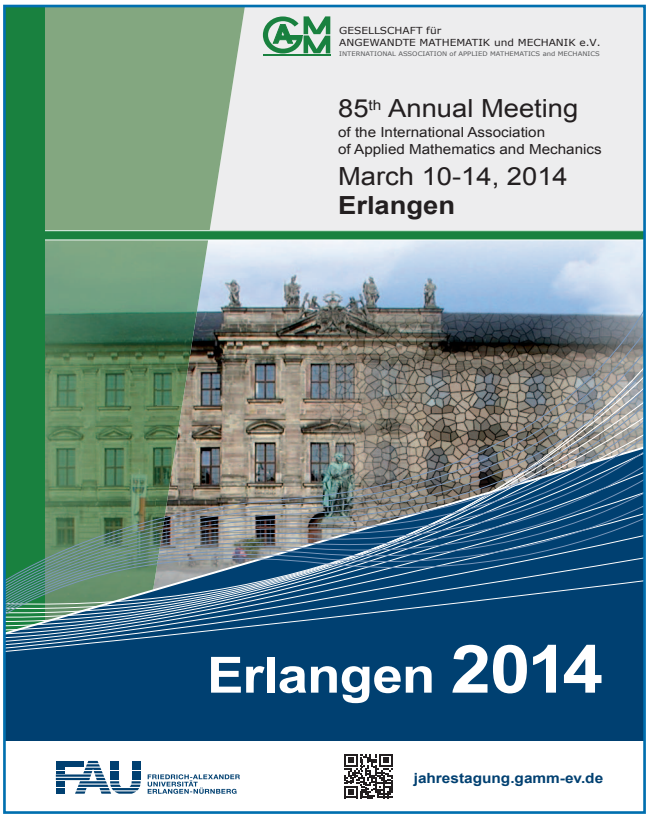

Local Organizing Committee

Paul Steinmann, Mechanics
Günter Leugering, Applied Mathematics

IMPORTANT DATES

Online registration starts September 9, 2013

Registration deadline for talks (Abstract upload)
December 13, 2013

Deadline for early registration fee
December 13, 2013

Deadline for payment in case an abstract has been submitted
December 31, 2013

End of online registration (after this date only on-site registration is possible)
February 14, 2014

Submission deadline for PAMM proceedings
May 31, 2014

the german association for
computational mechanics

Institute for Computational Mechanics
Technische Universität München
Boltzmannstrasse 15
D-85747 Garching, Germany
Phone: +49 89 289-15300
Fax: +49 89 289-15301
email: gacm@lnm.mw.tum.de
Internet: www.gacm.de